

See discussions, stats, and author profiles for this publication at: <https://www.researchgate.net/publication/372439747>

Reverse Engineering of the PRISMA Mission

Technical Report · May 2022

CITATIONS

0

READS

275

6 authors, including:



Giovanni Facchinetto

Beihang University

5 PUBLICATIONS 0 CITATIONS

[SEE PROFILE](#)



Davide Finco

Politecnico di Milano

4 PUBLICATIONS 0 CITATIONS

[SEE PROFILE](#)



Francesco Fabbri

Politecnico di Milano

3 PUBLICATIONS 0 CITATIONS

[SEE PROFILE](#)



Luca Giorcelli

Politecnico di Milano

2 PUBLICATIONS 0 CITATIONS

[SEE PROFILE](#)



POLITECNICO
MILANO 1863

Politecnico di Milano

Department of Aerospace Science and Technology

MSc Course of Space Engineering

**PRISMA Mission Reverse Engineering:
Space System Engineering and Operations
Final Report**

Team members:

Fabbri Francesco 102319-10643575
Facchinetti Giovanni 103235-10660994
Fereoli Giovanni 990939-10607373
Finco Davide 995524-10675826
Galeazzi Marco 991479-10622569
Giorcelli Luca 996226-10685512

Academic year 2021/2022

Contents

1	Introduction	1
1.1	Mission objectives	1
1.1.1	Primary objectives	1
1.1.2	Secondary objectives	2
2	ConOps	2
3	Functional Analysis	3
3.1	Functionalities	3
3.2	Mission risks	3
3.3	Mission drivers	4
4	Payloads	4
4.1	Payload constraints & requirements	5
5	Mission Analysis (MA)	6
5.1	Mission requirements	6
5.2	Orbit choice	6
5.3	Perturbation analysis	7
5.4	Environmental analysis	8
5.5	Launcher requirements	9
5.6	ΔV budget and maneuvers	10
5.6.1	Maneuvers overview	10
5.6.2	First Maneuver	10
5.6.3	Spacecrafts disposal	11
5.6.4	Experimental phase	12
5.6.5	GNC experiments overview	12
5.6.6	Examples of ARV maneuvers	14
5.7	Modes	16
6	Propulsive Subsystem (PS)	17
6.1	Generalities and requirements	17
6.2	Sizing method	18
6.3	Hydrazine engines	19
6.4	HPGP engines	21
6.5	MEMS engines (P/L)	22
7	Telemetry and Telecommand Subsystem (TTMC)	23
7.1	Generalities and requirements	23
7.2	Ground segment	23
7.3	Visibility analysis	23
7.4	Space segment	24
7.4.1	Architecture overview	24
7.4.2	Mango-OCC Link	25
7.4.3	Inter-Satellite Link (ISL)	26

7.4.4	Radio frequency Link	27
7.5	Link margins	28
7.6	Amplifier selection	29
7.7	Mass and power budget	29
8	Attitude Determination and Control Subsystem (ADCS)	30
8.1	Generalities and requirements	30
8.2	Disturbance torques analysis	31
8.3	Architecture and sizing	32
8.3.1	Mango (Main) ADCS	32
8.3.2	Tango (Target) ADCS	34
8.4	Mass and power budgets	34
9	Electrical Powers Subsystem (EPS)	36
9.1	Generalities and requirements	36
9.2	Architecture	36
9.3	Sizing	37
9.3.1	Power breakdown	37
9.3.2	Power storage	37
9.3.3	Power generation	38
9.3.4	Bus voltage	39
9.4	Mass budget	39
10	Thermal Control Subsystem (TCS)	39
10.1	Generalities and requirements	39
10.2	Architecture and sizing	40
10.2.1	Mango (Main) single node	40
10.2.2	Tango (Target) single node	41
11	Structural Subsystem (STR)	42
11.1	Generalities and requirements	42
11.2	Mango/Tango configurations	42
11.3	Sizing	44
12	Bibliography	46
13	Appendix	48
13.1	Mass and power s/s percentages	48
13.2	TTMTC theoretical charts	49
13.3	EPS theoretical charts	49
13.4	TCS theoretical charts	50
13.5	STR theoretical charts	50

1 Introduction

PRISMA mission aims to validate GNC technologies for autonomous formation flying, proximity operations, homing and rendezvous. These operations are fundamental for the future of space missions where the capability to perform correctly maneuvers such as in-orbit servicing or assembly, active space debris removal, deep space objects exploration is needed.

The mission is composed of two different satellites: the main ("Mango"), the only one able to communicate with Earth, and the target ("Tango").



Figure 1: Mango/Tango spacecrafts

1.1 Mission objectives

1.1.1 Primary objectives

The primary mission objectives are experiments regarding:

1. Autonomous formation flight (AFF) based on GPS and FFRF (Formation Flying RF) systems;
2. Homing and rendezvous (ARV) based on VBS only;
3. Proximity operations (PROX) based on GPS and VBS;
4. Final approach and recede operations (FARM) based on VBS only.

These four sets of experiments are selected because they highlight different important GNC capabilities and each of these is composed of several scenarios.

1.1.2 Secondary objectives

Secondary mission objectives are:

1. Flight demonstration of HPGP 1N thrusters;
2. Flight demonstration of the Micropropulsion System cold gas thruster;
3. SW & DHS demonstration: 100% fault-free operation of autocoded Model Based Software (MBSW), running on a LEON-3 processor, first full spacecraft flight operation of the RAMSES ground control system.

2 ConOps

Mango and Tango were launched together on *June 10th* 2010 into a Dawn-Dusk SSO orbit with 725 km of altitude. The basic mission was designed to have a total duration of 10-12 months. In the first two weeks, the satellites remained clamped together in order to commission and verify the correct behaviour of all the subsystems. After the separation of Tango the experimental phase started. This was designed to increase at each step activities complexity and to give early harvest results for each experiment; the purpose was to ensure experimental results to all experiments already at the beginning of the experimental phase and to avoid, in case of failures, the complete abortion of the mission.

Table 2. PRISMA Mission Timeline as from May 5 th 2010. DLR's related slots are shaded.						
Phase	Activity	Start [dd-mm-yyyy]	Finish [dd-mm-yyyy]	Duration [days]	Responsible	Usage
LEOP & Commissioning (57 d)	LEOP	15-06-2010	16-06-2010	2	SSC	-
	Combined Commissioning	17-06-2010	01-08-2010	46	SSC	-
	Tango Separation	02-08-2010	06-08-2010	5	SSC	-
	GPS Calibration	07-08-2010	10-08-2010	4	DLR	Primary
	HPGP 1	11-08-2010	14-08-2010	4	ECAPS	Primary
	Microthruster 1	16-08-2010	21-08-2010	6	NANOSPACE	Primary
	AFF Early Harvest	23-08-2010	07-09-2010	12	SSC	Primary
	VBS & FFRF Validation				DTU/CNES	Passenger
	FFRF Initialize	08-09-2010	10-09-2010	3	CNES	Primary
	AFC 1	13-09-2010	29-09-2010	17	DLR	Primary
Basic Mission (235 d)	FFRF Envelope	30-09-2010	09-10-2010	10	CNES	Primary
	VBS Long Range 1				DTU	Passenger
	HPGP 1/1	10-10-2010	11-10-2010	2	ECAPS	Primary
	PROX GPS 1	12-10-2010	21-10-2010	8	SSC	Primary
	ARV Coop	22-10-2010	31-10-2010	10	SSC	Primary
	FFRF GNC 1	01-11-2010	06-11-2010	6	CNES	Primary
	HPGP 2/2	07-11-2010	16-11-2010	8	ECAPS	Primary
	PROX GPS 2	17-11-2010	30-11-2010	10	SSC	Primary
	HPGP 3	01-12-2010	09-12-2010	7	ECAPS	Primary
	PROX/FARM VBS 1	10-12-2010	16-12-2010	5	SSC	Primary
	AFF Completion	03-01-2011	12-01-2011	8	SSC	Primary
	PROX/FARM VBS 2	13-01-2011	29-01-2011	13	SSC	Primary
	FFRF Passenger Near	10-12-2010	29-01-2011	18	CNES	Passenger
	FFRF GNC 2	01-02-2011	02-02-2011	2	CNES	Primary
	ARV Non-Coop	03-02-2011	02-03-2011	20	SSC	Primary
	FFRF Passenger Far				CNES	Passenger
	FFRF GNC 3	03-03-2011	06-03-2011	4	CNES	Primary
	AFC 2	07-03-2011	24-03-2011	18	DLR	Primary
Extended Mission (60 d)	Extra FF Experiment	25-03-2011	25-04-2011	22	tbd	Primary
	VBS Autonomous Navigation	27-04-2011	25-06-2011	60	DTU	Passenger
	HPGP 4	27-04-2011	26-05-2011	30	ECAPS	Primary
	VBS Long Range 2	27-04-2011	16-05-2011	20	DTU	Passenger
	DLR AOK	27-05-2011	25-06-2011	30	DLR	Primary

Figure 2: PRISMA Mission timeline

3 Functional Analysis

3.1 Functionalities

To sum up all the needed functionalities we report this list:

1. LEOP & Commissioning, especially GPS calibration;
2. Tango able to detach, detumble and control 3 DOF;
3. Tango able to communicate with Mango telemetry and GPS data;
4. Mango able to communicate with the ground for activities checking, data download and maneuvers command;
5. Good GPS coverage and Mango VBS/FFRF visibility of Tango;
6. Mango with a very precise 6 DOF guidance and control (FF & PROX), either autonomous or commanded by ground;
7. Mango capable of measuring HPGP and Microthrusters effects precisely;
8. Store experimental data between download windows;
9. Mango de-orbit with firings and Tango naturally due to perturbations within 25 years;

Since the mission is an on-orbit test bed for various kinds of experiments clearly the main focus is to guarantee the correct initialization and execution of the latter. Among all subsystems, the most important due to the main functionalities which should be granted are AOCS, OBDH and TELECOM. Principal functionalities clearly shall guarantee great guidance and navigation capability; but also the possibility to manage experimental data and interface with the ground station for downloading information and command operations.

3.2 Mission risks

After the timeline description, the group has identified a series of risks that can determine the failure of the mission.

Autonomous GNC software not correctly implemented A wrong implementation of the autonomous guidance laws can bring to a not precise formation and, in the worst case, to the Main and Target collision. A safe mode and the possibility to recognize failures autonomously are needed.

Information gap of relative navigation sensors Even with each subsystem nominally working and GNC software perfectly implemented, a malfunction of a relative navigation sensor could potentially ruin the mission. For instance, you have to guarantee: correct GPS calibration, Tango FFRF visibility and VBS non directly illuminated by the Sun.

Failures & non-nominalities A very high redundancy and FDIR system are needed to prevent any abort of the whole experimental phase. Ensuring results from all experiments at the beginning of the experimental phase, by increasing the difficulty over time, is another good strategy used.

Tango minimal HW Since Tango is needed only as a passive target it's provided with the minimum necessary hardware: it can't perform collision avoidance maneuvers or communicate with Kiruna without Mango.

3.3 Mission drivers

One of the main responsibilities of the system engineer is to guarantee the correct execution of each experimental case. In order to do that, a list of drivers for the design is established:

1. Perform correctly each experiment:
 - Attitude and Orbital Control Subsystem should be very precise and reliable.
 - GPS/VBS/FFRF should be able to provide excellent relative navigation information (GPS good coverage, VBS and FFRF should 'see' Tango).
 - Main and target Inter-Satellite Link to exchange information during 'cooperative' phases of experiments;
 - Robustness of software and control algorithms, especially for autonomous operations;
 - Avoid single point failures, reliable FDIR;
2. Stable and frequent OCC link to download experimental data, commands and check the correctness of maneuvers.

4 Payloads

A list of the payloads is summarized in the following table:

Hardware Flight Demonstrations	
HPGP Motor Tests	ECAPS
Microthruster Motor Tests	Nanospace
Relative GPS receivers	DLR
Vision Based Sensor (VBS)	DTU
RF Sensor Tests	CNES
LEON-3 on-board processor	OHB Sweden
PRIMA MEMs mass analyzer	IRF
Digital Video System	Techno Systems

Figure 3: Payloads summary

FFRF, HPGP and MEMS will be described in the specific subsections, while the other payloads are briefly mentioned here:

GPS The onboard GPS navigation system is contributed by DLR and provides the primary reference for absolute and relative position measurements. Each of the PRISMA satellites is equipped with a cold-redundant set of Phoenix GPS receivers. The receivers are cross-connected via a relay to a pair of GPS antennas on opposite sides of the spacecraft. In this way, GPS tracking can be ensured in all foreseen attitude modes of the PRISMA formation. During the flight, the spacecraft selects automatically the antenna to be used depending on the orientation of the antenna to maximize GPS constellation visibility.

VBS VBS is jointly developed by DTU and SSC. Use of the μ ASC (Micro Advanced Stellar Compass) of DTU, Lyngby, Denmark. The DTU star camera has the capability to track non-stellar objects and report the direction in global direction vectors. This capability shall be developed such that MAIN spacecraft can find the Target spacecraft from several hundred kilometers and deliver sufficient data in order to precisely determine the TARGET spacecraft's orbit (either on board or on the ground).

LEON-3 processor The DHS (Data Handling Subsystem) on Main employs a space-craft controller based on a LEON3-FT (Fault Tolerant) microprocessor (as OBC) from Aeroflex Gaisler. LEON3-FT implements a 32-bit processor compliant with the SPARC V8 architecture, which is particularly suited for embedded applications. LEON3-FT recognizes bit flips and is fault tolerant. It provides performance of about 20 MIPS and accommodates one FPU (Floating Point Unit).

DVS It's a compact digital video camera developed by Techno System Developments in Pozzuoli (Naples), Italy. The prime objective is to space-qualify the system and to demonstrate its performance in various applications. However, DVS is not linked to any navigation and control tasks of the PRISMA mission. DVS is installed on the MAIN S/C, it can be used to acquire images or video sequences related to the TARGET S/C during maneuvers.

4.1 Payload constraints & requirements

GPS requirements
<ul style="list-style-type: none"> • GPS shall be switched off during geomagnetic storms; • GPS shall have a pointing accuracy of at least 0.1 deg in a range of ± 20 deg along zenith direction; • GPS shall have at least two receivers capable of autonomous switching for better coverage.

VBS/FFRF requirements

- Tango shall have a brightness higher than a Mv7 star;
- Tango shall have LEDs for cooperative phases with Mango;
- Mango shall maintain Tango VBS contact during PROX/FARM/ARV experiments;
- Tango shall have an omnidirectional FFRF coverage;
- Mango VBS and FFRF shall be positioned on rendezvous direction;

HPGP/MEMS requirements

- HPGP/MEMS thrusters shall be positioned to guarantee free-torque motion;
- HPGP shall be a redundancy for the main propulsive system;
- Mango GPS and Accelerometers shall have a resolution of at least TBD m and TBD m/s^2 respectively;

5 Mission Analysis (MA)

5.1 Mission requirements

Main/Target mission analysis requirements

- Mango/Tango orbit shall guarantee a coverage rate of TBD passages/day with a coverage duration of at least 8 minutes over Kiruna Ground Station;
- Mango/Tango orbit shall guarantee a low radiation environment and maximize lighting conditions;
- Mango/Tango orbit shall guarantee at least 1 year of lifetime;
- Mango/Tango orbit shall be compatible with launcher capabilities.

All these points will be satisfied by the chosen orbit.

5.2 Orbit choice

The selected orbit for the mission is a Dawn-Dusk Sun-Synchronous with an apogee of 780 km and a perigee of 720 km altitude. Keplerian elements taken on *June 15th 2010* are:

a [km]	e [-]	i [deg]	Ω [deg]	ω [deg]	θ [deg]
7089.36	0.002	98.28	353.90	8.628	351.49

This orbit is a good choice for this mission because, since it is only needed to perform GNC experiments, the EPS and TCS subsystems design can be simplified. Sun direction will always be the same and eclipse phases will be minimized (max 20 min/day 80 days/year). Moreover, the light-sensitive devices, like the VBS and the star trackers, are easier to point to work in the best possible scenario. Furthermore, a LEO with 700 km altitude is a trade-off between perturbations (e.g Tango shall not de-orbit too quickly), orbital period, communication and launch capability.

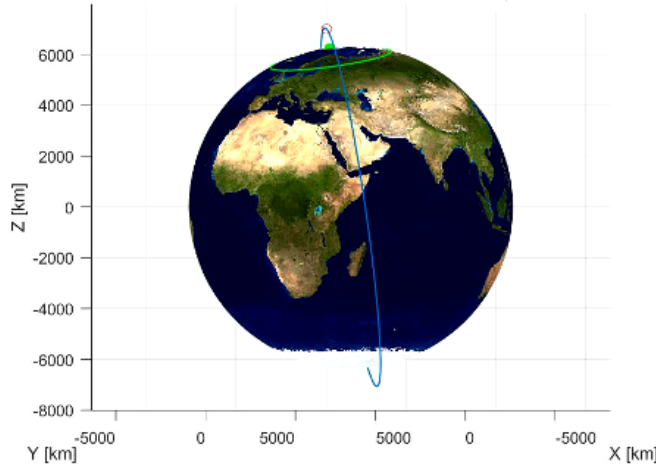


Figure 4: Spacecrafts orbit

5.3 Perturbation analysis

Starting from known formulas, the group has been able to compute the following orders of magnitude for the perturbations of the SSO orbit: $J2 \sim 10^{-5} \text{ m}^2/\text{s}$, $SRP \sim 10^{-8} \text{ m}^2/\text{s}$, $Aerodynamic Drag \sim 10^{-8} \text{ m}^2/\text{s}$.

The evolution of the orbital elements of TANGO (from *space-track.org*) can be seen below:

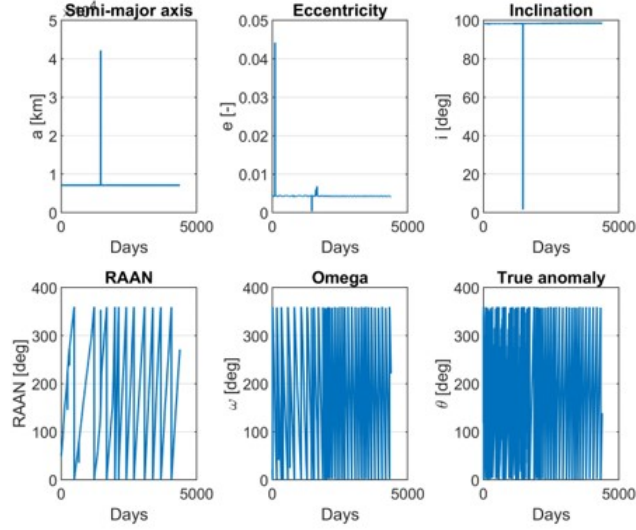


Figure 5: Tango (Target) ephemeris

From these plots it can be confirmed that the most critical disturbance is the J2 effect: RAAN regression and perigee precession are clear, while the semi-major axis and eccentricity variations are negligible. Moreover, being in LEO we can say that the third body

perturbation of the Moon is irrelevant.

Notice that the SSO orbit is obtained by exploiting the J2 effect. Knowing some parameters of the orbit, it is possible to compute (so to cross-check) the inclination needed to have RAAN regression equal to Earth/Sun rotation ($\dot{\alpha} = 1.991 \cdot 10^{-7} \text{ rad/s}$):

$$\frac{\Delta\Omega}{T} = \dot{\alpha} \rightarrow \cos i = -\frac{\dot{\alpha} T p^2}{3\pi J2 R_E^2} \rightarrow i = 98.26 \text{ deg}$$

5.4 Environmental analysis

Along the spacecraft's orbital path atomic oxygen (AO), ultraviolet (UV) radiation and ionizing radiations (TID/DDD and SEE) are the main deterioration causes of materials and electronic components. Due to the presence of much orbital debris, the design of collision avoidance procedures and the use of materials resistant to low-energy impacts are needed. Therefore the following graphs shall be taken into account during components sizing (solar panels, shielding, thermal coating and so on):

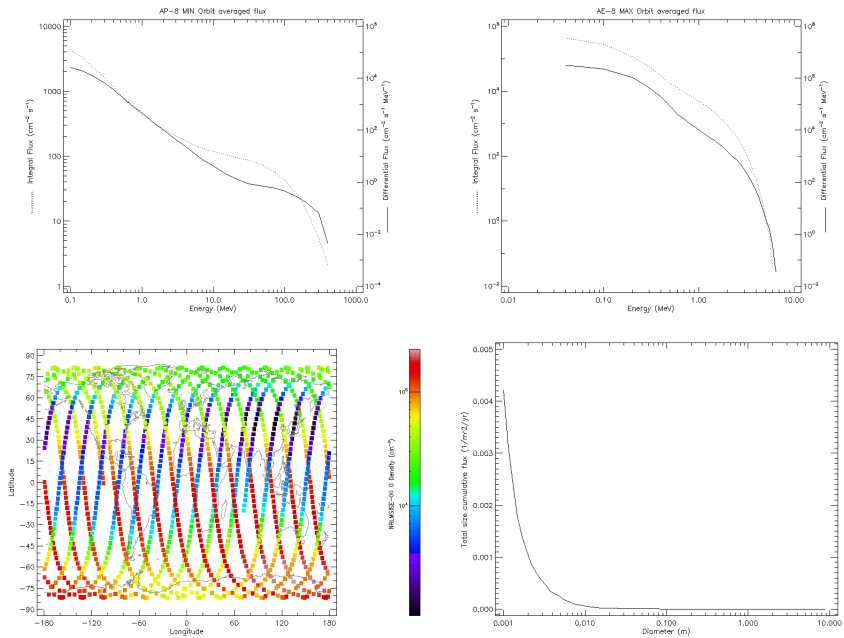


Figure 6: Protons, Electrons, AO density and Debris flux

During the flight, GPS disturbances must be considered: over the South Atlantic Anomaly or during Sun Proton Events its measurements are not reliable. In the case of the mission, Aurora can be experienced when the spacecraft is over the poles, due to the high inclination of the orbit.

Plasma charging and low outgassing criteria from ECSS must be considered. In order to do so, the design shall satisfy many requirements: ECSS-E-ST-20-07CRev.2 in order to avoid charging/sputtering/contamination due to ionospheric plasma and ECSS-Q-70-02A to not have a vacuum-caused loss of material and deterioration zones.

Looking at the 'R sunspots number - time' chart, it can be noticed that the solar activity during 2010 had a minimum. In that period, which corresponds roughly to the nominal mission, the 24th solar cycle had just begun. This is an important aspect to be taken into account in the design of the mission, since solar activity influences:

- Earth atmosphere (AO, density, temperature...);
- Avionics (especially GPS) due to SPE, CME and other Sun events;
- Material degradation due to LET/NIEL.

5.5 Launcher requirements

Mass budget During preliminary analysis Picard, Mango and Tango wet masses (spacecrafts, DMM/PLM/SLM margins and propellant/pressurant masses) resulted:

$$\begin{cases} m_{Picard,wet} = 150 \text{ kg} \\ m_{Mango,wet} = 145 \text{ kg} \\ m_{Tango,wet} = 40 \text{ kg} \end{cases}$$

So the wet mass resulted $m_{nominal,wet} = 335 \text{ kg}$. Considering also an additional MLM margin of 25% the resulting mass at launch (adapter mass will be directly subtracted from launchable one) is: $m_{launch} = 418.75 \text{ kg}$.

Stack dimensions The dimension of the spacecrafts are:

$$\begin{cases} dim_{Picard} : 700x800x1100 \text{ mm} \\ dim_{Mango} : 800x800x1300 \text{ mm} \\ dim_{Tango} : 800x800x300 \text{ mm} \end{cases}$$

So the selected stack will be $800x800x2700 \text{ mm}$.

Launcher choice

Launcher requirements

- Launcher capabilities shall be able to satisfy also PICARD mission requirements;
- Launcher performance shall guarantee Picard and Mango/Tango spacecrafts injection on their nominal orbits;
- Launcher fairing envelope shall be able to lodge correctly Picard and Mango/Tango packed together.

Among all possibilities, the Russian DNEPR was the best choice in terms of Cost/Kg-Performance. In fact:

- The launchable mass (with a 75 kg adapter and the correct fairing) is 450 kg;
- The chosen fairing envelope has a maximum height of 4310 mm and the total height of Mango, Tango and Picard together is 2700 mm.

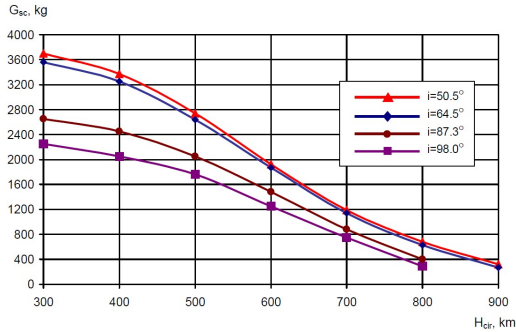


Figure 4.1-3 Dnepr-1 Performance Curves for Circular Orbits

Figure 7: DNEPR performances

5.6 ΔV budget and maneuvers

5.6.1 Maneuvers overview

A total $\Delta V = 180 \text{ m/s}$ of the main propellant is allocated for the entire mission, where¹:

$$\begin{cases} \Delta V_{Hydrazine} = 120 \text{ m/s} \\ \Delta V_{HPGP} = 60 \text{ m/s} \end{cases}$$

These data come from literature, now let's take a look more in-depth at their taxonomy and what it can be said about them. At first, it is useful to determine the amount of propellant used for the initial orbital correction and the final disposal, then the experiments assigned ΔV can be correctly evaluated.

5.6.2 First Maneuver

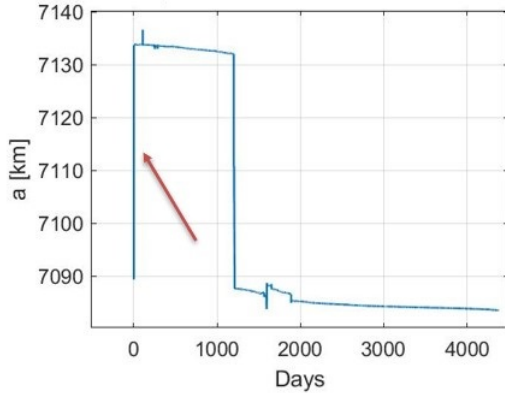


Figure 8: Mango (Main) semi-major axis variation during first orbital correction

Looking at the ephemeris, it can be observed that on 17/6/2010 Mango (with Tango clamped) performed the first maneuver to put the couple of S/C on their defined orbit. The maneuver consisted of a variation of the semi-major axis from 7089 km to 7133 km. Assuming a Hohmann's Transfer the total cost resulted in $\Delta V_{corr} = 23 \text{ m/s}$.

¹MEMS propulsive system has a negligible ΔV capability.

5.6.3 Spacecrafts disposal

Mango disposal Around 2015, after a not initially planned Picard inspection, Mango performed a disposal burn to decrease its semi-major axis to exploit more aerodynamic drag orbital disturbance. Looking at the Keplerian elements variation in time and doing a simple Hohmann's transfer the total cost resulted in $\Delta V_{disp} = 1.22 \text{ m/s}$.

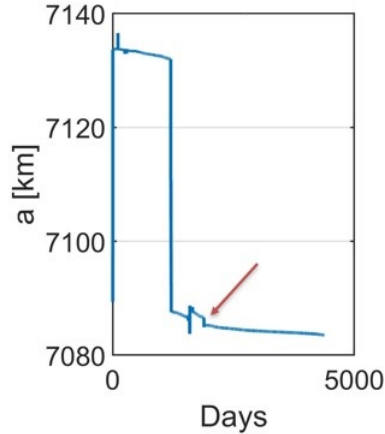


Figure 9: Mango (Main) semi-major axis variation during disposal burn

After this maneuver its re-entry is planned in 30 years; this value is obtained from literature knowing Mango ballistic coefficient.

Tango disposal Tango does not have any kind of propulsion system to lower its orbit. Given its altitude in 2015, from the following chart and knowing its mass/area ratio (about 110 kg/m^2), the de-orbit time is about 110 to 150 years. This result is proven by the TLE of the s/c in which it can be seen a very slow semi-major axis decreasing.

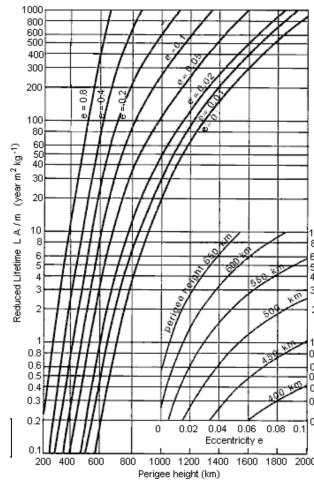


Figure 10: De-orbit time chart

Notice that ESA space debris policies about de-orbiting within 25 years from the end of the mission were published a few years after the PRISMA mission and so in this case they are clearly non-respected.

5.6.4 Experimental phase

Now after a direct estimation of deterministic costs, it is possible to evaluate backward stochastic ones (considering relative margins). Remember that deterministic maneuvers need a 10 m/s of margin and stochastic ones 100%. Hence the allocated propellant should be:

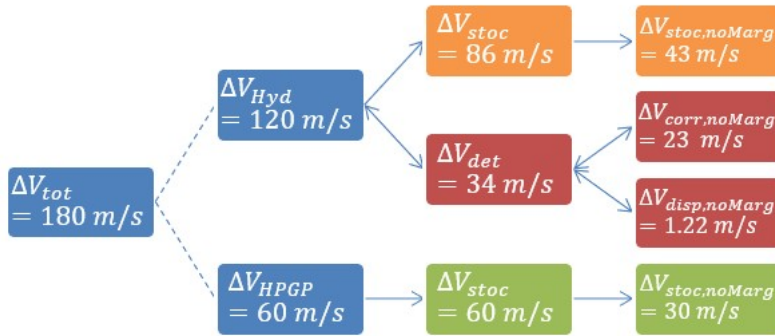


Figure 11: ΔV allocation

These values shall be compared with the real used amount of Hydrazine and HPGP. In the real mission, a total ΔV of 50 m/s of Main propellant remains at the end of the nominal mission (Aug. 2011)². This is in line with what has been computed: the sum of stochastic ΔV with no margins and the initial maneuver one gives us the same result. The same reasoning is applied with HPGP where at the end of the mission around 30 m/s of propellant remained. Leftovers were then used for external partners' missions.

5.6.5 GNC experiments overview

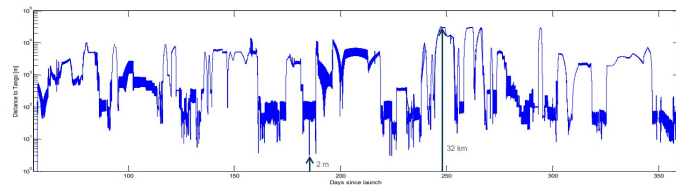


Figure 12: Distances Main/Target - Time

²Bodin, P. et al., "The PRISMA Formation Flying demonstrator. Overview and Conclusions from the main mission", Proceedings of the 35th annual AAS Guidance and Control Conference, February, Breckenridge, Colorado, 2012.

In this section, all the main sets of GNC experiments performed by Prisma up to 31st December 2011 are described.

Autonomous Formation Flight AFF, between 5000-20 m and using GPS/FFRF, is used to test closed-loop autonomous formation acquisition, guidance/control laws and support of other GNC experiments by maintaining and reconfiguring the formation between them. Inside the AFF experiment, there is SAFE by DLR: a fuel-optimized set of 22 formation flying formations between 2000-100 m, it lasted 6 weeks and used 5 m/s.

Autonomous Rendezvous ARV, between 100000-3 m and using VBS, emulated rendezvous in GEO, assembly in escape orbits and Mars sample return scenarios.

ARV is the set of experiments that used the biggest amount of propellant for each maneuver. AFF needs just to counteract disturbances to maintain the formation and PROX-/FARM were between very small distances, so their ΔV were in the order of mm/s and it was very complex to keep track of. For this reason in the next section, two examples of Homing/Rendezvous and an example of FARM (described below) are analyzed for comparison.

Proximity Operation PROX, between 100-3 m and using GPS/VBS, demonstrated on-orbit servicing/inspection/assembly around large and virtual structures. Moreover, PROX with VBS can be characterized by two different conditions of the target: cooperative (by using LEDs aid) or non-cooperative Target. In these operational phases, the VBS delivers both the relative distance and the relative attitude to the target spacecraft.

Final Approach and Recede Maneuvers FARM, between 3-0 m and using VBS, simulated approach as close as possible to demonstrate on-orbit servicing, inspection and assembly.

5.6.6 Examples of ARV maneuvers

In this section two ARV maneuvers and then a FARM one are simulated to compare ΔV . The first two are modeled using State Transition Matrix (STM) theory, and the last one through simplified formulas from theory.

Long-range out-of-plane Homing (30-3 km along-track)

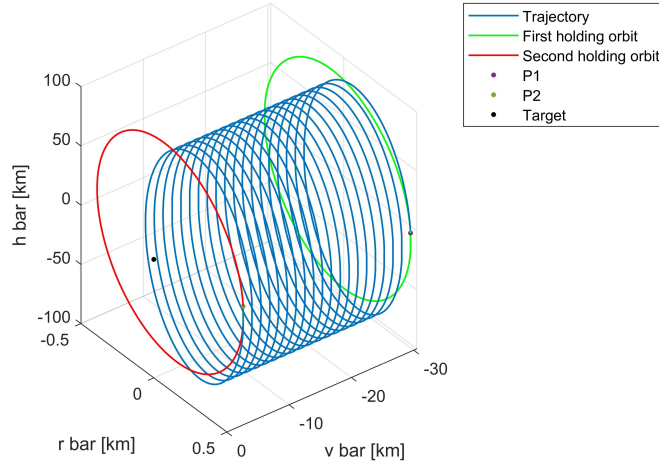


Figure 13: Mango (Main) homing maneuver trajectory

This maneuver aims to test line-of-sight homing, in real operational cases, VBS would retrieve also Tango attitude. Moreover, it's very safe since $\delta e \parallel \delta i$. The maximum radial distance is reached when it intersects the target orbital plane. Results are³ for $[-29.5, 0.5]$ km to $[-2.95, 0.5]$ km:

$$\Delta V_{hom} = 1.21 \text{ m/s}$$

$$ToF_{hom} = 31.24 \text{ h}$$

Results shown here are perfectly fine compared with the ARGON mission by DLR:

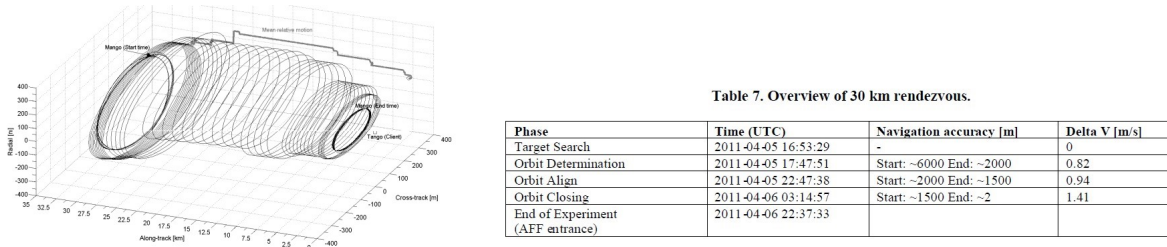


Figure 14: ARGON experiment trajectory and data

³An infinitesimal trigger velocity component out-of-plane is needed.

This maneuver design is driven by the usage of VBS as a relative navigation sensor. In order to use a camera for maneuvers, it is better to employ a little bit more propellant, and have a relative motion also out of the plane ($\delta i \neq 0$) in order to see the target from each side and avoid rotation resonance problems. This maneuver's real values are approximately $\Delta V = 3 \text{ m/s}$ and the $ToF = 30 \text{ h}$ ⁴, but it should be considered the fact that it is done in different steps. The initial condition is an offset of 30 km along-track.

Short-range in-plane Rendezvous (10-0.1 km along-track) This one is more traditional but less safe and more attitude demanding to maintain target on camera FoV. From $[-10, 0] \text{ km}$ to $[-0.1, 0] \text{ km}$:

$$\Delta V_{rv} = 14 \text{ cm/s}$$

$$ToF_{rv} = 17.95 \text{ h}$$

Clearly, this maneuver is less expensive than the previous one.

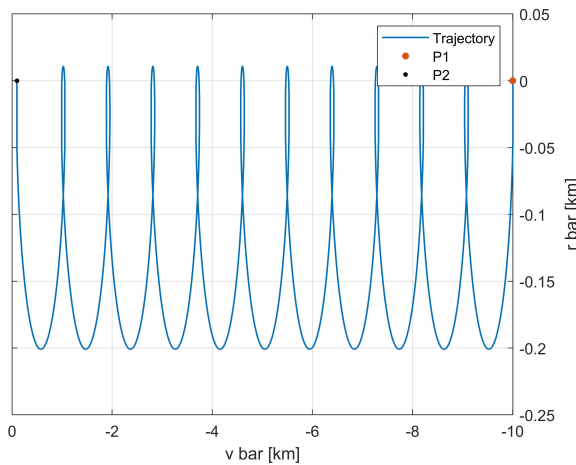


Figure 15: Mango (Main) rendezvous trajectory

Unfortunately, it's only cited in literature but not described or shown even partially, so it is impossible to make comparisons.

V-Bar Approach (50-3 m along-track) It shows the nominal cost PROX&FARM operations, hence mm/s maneuvers. Compared to previous maneuvers it's clear that these ones shall be considered not singularly but cumulatively. In this case, continuous control along the r-bar is needed due to coupling with holding point burns on v-bar. Results for $[50, 0] \text{ m}$ to $[3, 0] \text{ m}$ are:

$$\Delta V_{app} = 2\Delta x + 2\omega\Delta\dot{x}\Delta T = 119.2 \text{ cm/s}$$

$$ToF_{app} = 1.31 \text{ h}$$

⁴Notice that maneuvers are designed to be as cheap as possible to perform more experiments, that's why times of flight are always relatively high.

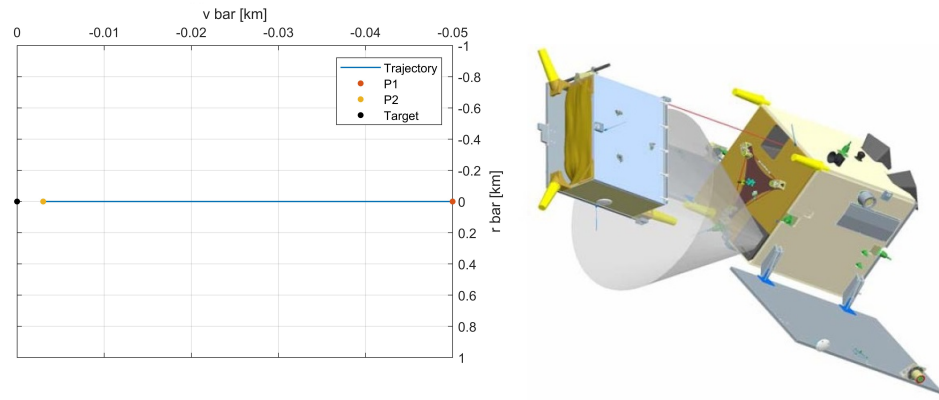


Figure 16: Mango (Main) along-track approach trajectory

Noticed that here it is represented a v -bar approach, but depending on the mode Mango/Tango performed also some r -bar ones.

5.7 Modes

Mango and Tango GNC modes are designed to support all the experiments with the maximum level of generality. While Tango has only the possibility to point either the Sun or nadir direction, Mango modes are designed to also fulfill the experimental needs of the mission. In fact Mango, besides two safe modes like Tango, has seven other ones: manual mode for command by ground maneuvers/ trigger experiments while the other six are dedicated to a specific experiment (different GNC control laws).

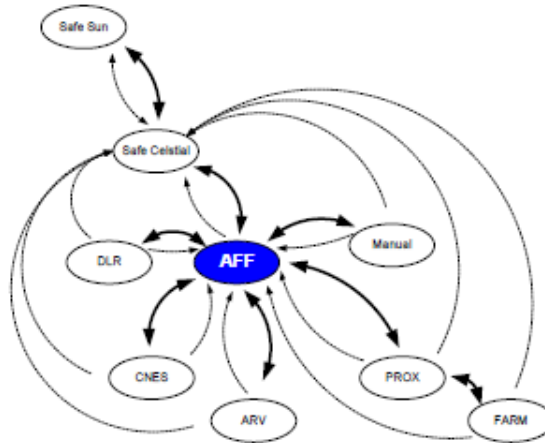


Figure 17: GNC modes overview, solid lines indicate ground triggered and dashed lines autonomous ones.

The first modes used by both spacecraft after the launch was Safe Sun in order to guarantee all the minimum functionalities with the minimum hardware required and minimum

power consumption (Mango uses only sun sensors and magnetometers). After the commissioning phase, Mango switched to a more hardware-demanding safe mode called Safe Celestial where it used also star trackers for better pointing and higher accuracy.

The modes architecture is designed such that the Autonomous Formation Flying (AFF) experiment mode is the central one from which all other modes can be triggered. AFF has been chosen for this role since it is the most flexible and is capable of maintaining and reconfiguring spacecrafts between experiments. This mode is highly autonomous, requires limited ground intervention and ensures safety conditions for both spacecrafts.

A large amount of time is spent in Manual mode due to the fact that all HPGP/MEMS experiments use this mode: the objective is not formation flight but the qualification of new technologies. The relatively small amount of time spent in proximity operations is due to the short duration of such forced motion experiments.

6 Propulsive Subsystem (PS)

6.1 Generalities and requirements

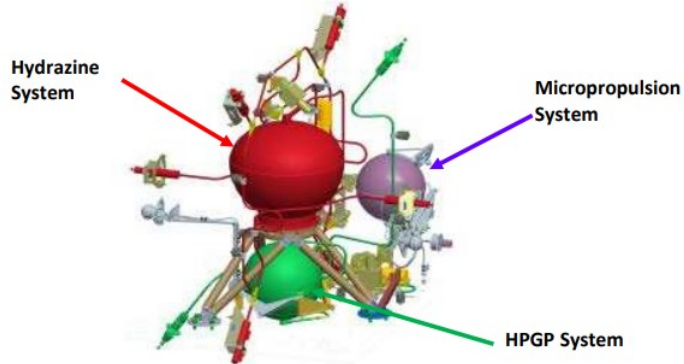


Figure 18: Overall propulsive subsystem

Only Mango has a propulsive system. Tango instead serves only as a target and therefore its architecture is minimized. HPGP and MEMS propulsive systems are a technological demonstration and so they were not directly considered during the design phase; despite that, the discussion deals with their sizing for the sake of completeness.

Main propulsive s/s requirements

- Propulsive system shall be able to control 3 DoF (only CoM, torque-free motion) with a 1N force to perform relative GNC experiments;
- Mango PS shall be pulsable with TBD MiB;
- Mango PS shall have $\Delta V = 120 \text{ m/s}$
- Mango PS shall have at least 1 year of qualified operational life and be highly redundant;
- Mango PS shall not have thrusters rendezvous direction.

A simple Hydrazine (N_2H_4) based monopropellant system can meet all these requirements: electric propulsion lacks of authority and simplicity, while bi-propellant ones of weight and fine control capability. A monopropellant propulsive system grants both relative orbital control and precise station keeping: the first aim is to guarantee a range of thrust [$mN - N$] in order to perform all the relative GNC experiments required (FF, ARV, FARM, PROX).

Moreover, HPGP hardware will cover also redundancy requirements and it will give the possibility to extend the mission if needed after Hydrazine runs out. MEMS instead has no ΔV capability and it can be used only for experiments on itself.

The propulsive system influences many aspects of Mango design: TCS (heaters and avionics are heat generation sources), EPS (valves, sensors and heaters power budget), OBDH (sensors), STR(tanks and thrusters positioning) and mass/inertia matrix variation.

6.2 Sizing method

The procedure for a phase 0/A sizing of Hydrazine and HPGP propulsive systems is the same; now it is reported the workflow of the latter, the one for the MEMS subsystem is slightly different and it will be reported in the relative subsection. Considering ESA margins, computations are:

- Propellant quantity sizing:
 - With Tsiolkovski's equation the propellant mass is computable, considering also 2.5% (MAR-MAS-080) of ullage and loading uncertainties:

$$M_{prop} = 1.025 \cdot M_0 \left(1 - e^{\frac{\Delta V}{I_{sp} g_0}}\right)$$

- Propellant volume with 10% (MAS-CP-010) for unusable volume:

$$V_{prop} = 1.1 \cdot \frac{M_{prop}}{\rho_{prop}}$$

- Pressurant sizing:
 - Knowing chamber pressure range and assuming the losses fixed ($\Delta P_{inj} = 30\% P_{chamb}$ and $\Delta P_{lines} = 50 \text{ kPa}$) it is possible to compute:

$$P_{tank,in} = P_{chamb,in} + \Delta P_{inj} + \Delta P_{lines} \quad P_{tank,fin} = \frac{P_{tank,in}}{B}$$

- Now the gas mass can be computed with 20% of margin (MAR-MAS-090) and volume needed at the beginning:

$$V_{gas,in} = \frac{V_{prop}}{B - 1} \quad m_{gas} = 1.2 \cdot \frac{P_{tank,in} V_{gas,in}}{R * T_{cc}}$$

- Tank sizing:

- Tank volume and radius (assumed spherical) are:

$$V_{tank} = V_{gas,in} + V_{prop} \quad r_{tank} = \left(\frac{3}{4\pi} V_{tank} \right)^{\frac{1}{3}}$$

- Considering Aluminium (Al7075)⁵ as tanks material ($\rho_{tank} = 2810 \text{ kg/m}^3$ and $\sigma = 503 \text{ MPa}$):

$$t_{tank} = \frac{P_{tank} V_{tank}}{2\sigma} \quad m_{tank} = \rho_{tank} \frac{4}{3}\pi ((r_{tank} + t_{tank})^3 - r_{tank}^3)$$

- Assuming thruster mass equal to 0.38 kg as MONARC-1, the dry mass of the propulsive system without pipes weight is:

$$m_{PS} = m_{tank} + m_{gas} + n_{nozz} \cdot m_{nozz}$$

6.3 Hydrazine engines

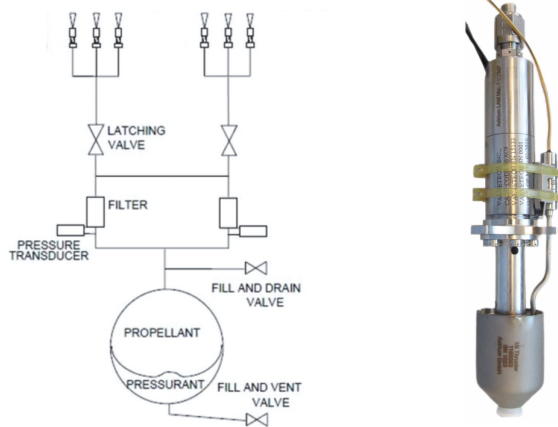


Figure 19: Hydrazine (Main) propulsive subsystem

Useful data from mission requirements and real datasheets are:

ΔV [m/s]	I_{sp} [s]	m_{dry} [kg]	$m_{prop,real}$ [kg]	$P_{single,thrust}$ [W]
120	225	6.08	11	18

P range [bar]	P_{BOL} [bar]	T range [N]	B ratio [-]
[4.8-27.6]	19	[0.32-1]	4:1

Instead, the propellant and pressurant properties are:

⁵Titanium can't be used as tanks material in LEO due to its high melting temperature, it's not compatible with atmospheric disposal.

Propellant [-]	ρ [g/cm ³]	Pressurant [-]	R^* [J/(kg K)]	γ [-]
Hydrazine	1.01	Helium	2077	1.660 (20°C)

The architecture is composed by:

- Two fill and vents valves for gas and liquid loading, two flow control valves (FCV), two pressure transducers and two filters;
- Single spherical aluminum tank (Hydrazine compatible) equatorially attached;
- Blow-down pressurization system with an elastomeric diaphragm. That choice is made to reduce weight and complexity by accepting a loss of performance during usage.

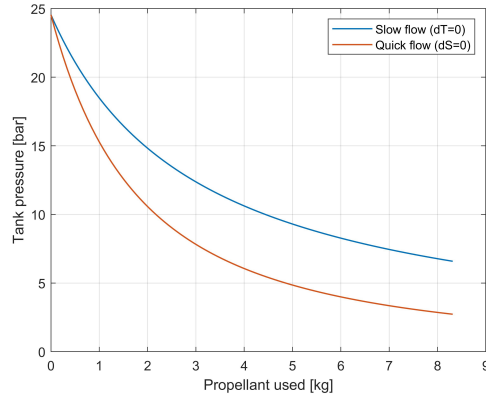


Figure 20: Blow-down pressurization performance

- Six 1-N thrusters with heated catalytic beds arranged as two centered on $\pm Y$ panels and four on the edges between $\pm X, \pm Z$ panels. All thruster projections pass through CoM and guarantee free-torque translational motion without being along rendezvous direction. The number is driven also by redundancy purposes.

Referring to the previously described workflow results are:

m_{prop} [Kg]	m_{gas} [Kg]	r_{tank} [cm]	t_{tank} [cm]	m_{tank} [Kg]	m_{PS} [Kg]
8.11	0.0149	14.27	0.037	0.2568	2.55

The sized mass of the propellant is quite precise with respect to the real one, instead, the sized propulsive system mass has some problems. The computations made include only thrusters, tank and pressurant mass without taking into consideration: tank attachments (from literature $\sim 20\% m_{tank}$) and bladder, feeding pipes, filters and different types of valves, sensors and electrical components. In fact for instance a latch valve could weigh on its own ~ 500 g⁶.

⁶<https://www.space-propulsion.com/brochures/valves/space-propulsion-valves.pdf>

6.4 HPGP engines

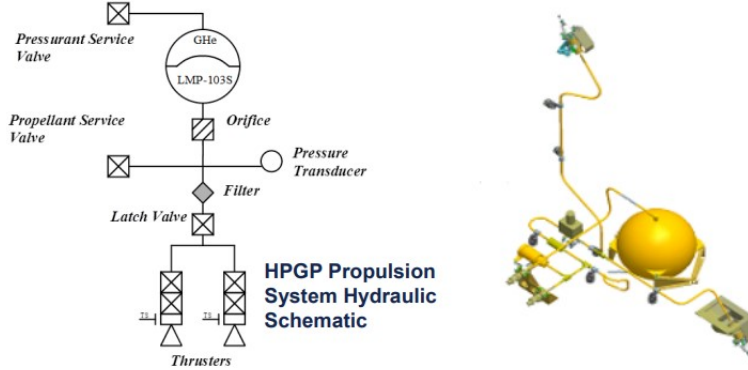


Figure 21: HPGP propulsive subsystem

Useful data from mission requirements and real datasheets are:

ΔV [m/s]	I_{sp} [s]	m_{dry} [Kg]	$m_{prop,real}$ [Kg]	Power [W]
60	225	3.9	5.4	8

P range [bar]	$P_{in,0}$ [bar]	T range [N]	B ratio [-]
[4.5-22]	18.5	[0.25-1]	3.8:1

Instead, the propellant and pressurant properties are:

Propellant [-]	ρ [g/cm ³]	Pressurant [-]	R^* [J/(kg K)]	γ [-]
LMP-103S	1.24	Helium	2077	1.660 (20°C)

The architecture is very similar to the previous one, the only difference is that since the HPGP system is a payload, there are only two 1N thrusters positioned on opposite short edges between $\pm X$, $\pm Z$ panels and passing through CoM.

Now from computations:

m_{prop} [kg]	m_{gas} [Kg]	r_{tank} [cm]	t_{tank} [cm]	m_{tank} [Kg]	m_{PS} [Kg]
4.58	0.0086	11.76	0.0287	0.1408	0.9094

The computed dry mass doesn't contain some non-negligible components, so its value is quite different from the one found in the literature, as for the previous case.

6.5 MEMS engines (P/L)

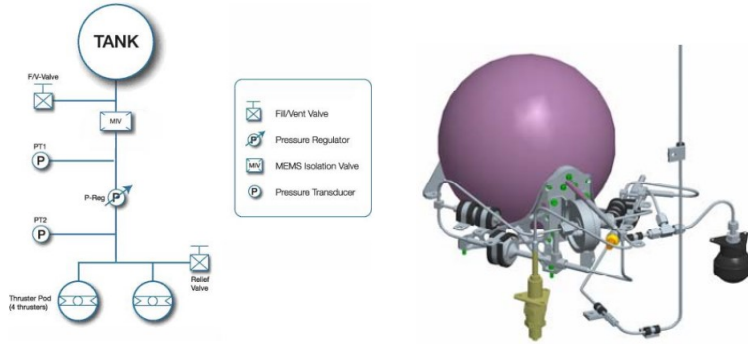


Figure 22: MEMS propulsive subsystem

The Micro Electro Mechanical System (MEMS) is a cold gas propulsive system. It has 2 pods of 4 thrusters at 90° on $\pm Z$ panels equipped with heaters to improve performances (I_{sp} in the table below is given under cold and hot modes). The architecture also includes a high-pressure tank, a filter, two pressure transducers, a pressure regulator, a pressure relief valve, and a gas fill/vent valve.

Since for this specific engine we did not find key data, we decided to try to size it starting from some data and approximations. We found the following data:

I_{sp} [s]	P_{in} [bar]	Propellant	R^* [J/(kg K)]	γ [-]
50-100	4	N_2	296.8	1.40

Some assumptions are made: $r_{tank} = 10\text{ cm}$ (visual comparison with HPGP tank), Aluminium (Al7075) tank and a Blowdown Ratio $B = 4$. Using the inverse procedure with respect to what has been used for the main propulsive subsystem, the results are the following:

ΔV [m/s]@cold,hot mode	$m_{propellant}$ [kg]	t_{tank} [mm]	m_{tank} [kg]	m_{budget} [kg]
0.36-0.73	0.11	0.23	0.08	1.05

Unfortunately, it is not possible to compare these results with real ones, but they make sense compared to Hydrazine/HPGP subsystems.

7 Telemetry and Telecommand Subsystem (TTMC)

7.1 Generalities and requirements

Since the PRISMA mission is an experimental mission with the purpose of demonstrating the functionality of a wide range of GNC maneuvers and some new propulsive systems, scientific data will be mostly telemetry. Requirements for TT&C subsystem design are:

Main/Target TTMC requirements

- Mango (Main) shall have a direct downlink/uplink with Kiruna Ground Station;
- Mango (Main) links with GS shall be at 2120-2300 MHz with at least 1 Mbit/s downlink and 4 kbit/s uplink;
- Tango (Target) shall use Mango (Main) as relay satellite;
- Mango (Main) and Tango (Target) shall have an Inter-Satellite Link at 450 MHz working between 0.5-10 km and with at least 15 kbit/s downlink/uplink;
- Mango (Main) and Tango (Target) shall have an RF Link at 2275 MHz working between 0.5-30 km and with at least 12 kbit/s downlink;
- Eb/N0 and SNR of each link shall be higher than TBD dB and TBD dB respectively with a 3 dB margin;
- BER (Bit Error Rate) shall be at least 10^{-6} for each link;

7.2 Ground segment

PRISMA mission is led by Swedish Space Corporation, therefore the mandatory ground station is located in Kiruna (ESTRACK). A second site would be too expensive and, due to its latitude of 67°53' N, it's also not needed. Kiruna has a 13-meter diameter S-band antenna with:

Frequencies [MHz]	Tx: 2025-2120 - Rx: 2200-2300
Antenna Gain [dBi]	Tx: 46 - Rx: 48.6
Noise T [K]	93

7.3 Visibility analysis

TT&C subsystem design is mostly driven by mission analysis: the chosen orbit in fact determines access time and transmission delay, therefore also data-rate R and OBDH design. Taking into account a 5° minimum elevation angle (MAR-COM-090, e.g. for atmospheric perturbations and soil morphology) and the desired orbit altitude, the spacecrafts visibility geometry is ⁷:

$$T_{average,vis} = 0.8 \quad T_{max,vis} = 0.8 \Delta\sigma_{max} \sqrt{\frac{a_{orb}^3}{\mu_{Earth}}} = 9.8 \text{ min}$$

⁷The $T_{max,vis}$ is found when the spacecraft passes exactly over the Kiruna Ground Station. Since the real field of view is a cone it is obvious that $T_{max,vis}$ is not the nominal time of visibility: in general, it should be considered an average time.

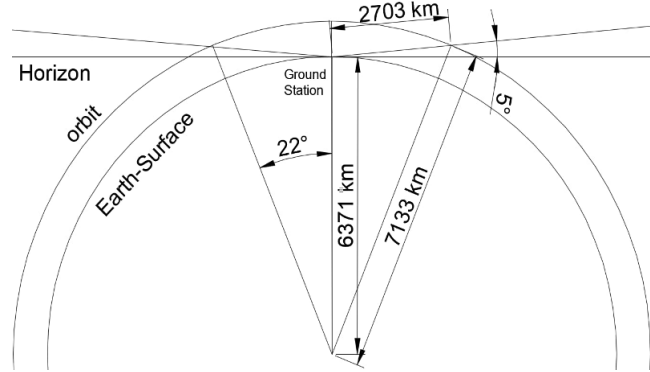


Figure 23: Visibility Mango(Main)-OCC geometry

$$S_{Tx/Rx, \text{worst}} = 2703 \text{ km}$$

Moreover, due to mission analysis, PRISMA spacecrafsts perform 14 revolutions/day of which only 10 are visible from Kiruna OCC. Of those, 6 were used for active flight operations (Telecommand/Navigation, Uplink), and 4 for downloading data (Telemetry/- Science, Downlink). Notice that this situation is valid only in the first part of the mission: Tango can't counteract its CoM disturbances and so Keplerian Elements constantly change during the mission.

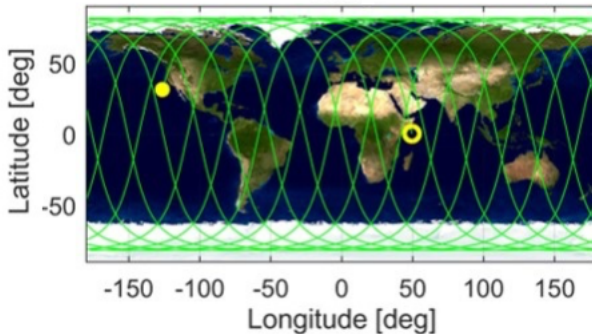


Figure 24: Mango(Main) ground track in 24 hours

7.4 Space segment

7.4.1 Architecture overview

The choices adopted for the TTMC architecture of the two satellites are:

- Mango-OCC link is based on a *Store&Forward* approach: data is stored by OBDH s/s during transmission delays and later, once the link is established, sent.
- Tango, in order to minimize its power budget, is designed with only an Inter-Satellite Link (ISL) with Mango which should work between 0.5-10 km. FFRF (a payload) will serve as redundancy.

TTMC subsystem will put some requirements mostly on EPS (power consumption), OBDH design (data storage) and TCS (heat source).

7.4.2 Mango-OCC Link

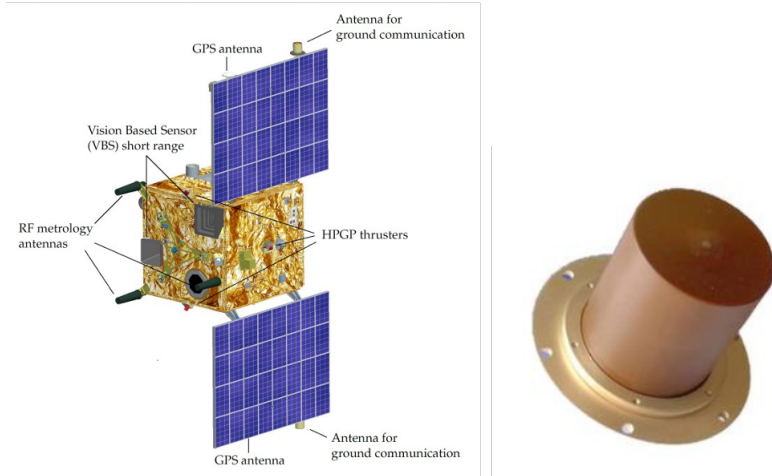


Figure 25: Mango(Main)-OCC link architecture

This link shall work in S-band and since we are in LEO⁸ we would like to have an almost spherical coverage (less pointing requirements). A good strategy is, adding also redundancy, to put a hemispherical transmitter on the edge of both solar panels. For this purpose two S-band Helix antennas with $G_t \sim 1.5 \text{ dB}$ (large beam-width so short antennas) have been chosen.

In the tables below a summary of down-link (Main Helix antenna) and up-link (Kiruna OCC parabolic antenna) characteristics are presented:

	R [kbit/s]	P_t [dBm]	G_t [dBi]	G_r [dBi]	S_{worst} [km]	f [MHz]
D/L	10^3	33	1.5	48.6	2703	2200
U/L	4	54.77	46	1.5	2703	2100

Antenna sizing It is possible to size the antenna using some experimental formulas from literature (Figure 40) knowing the antenna type. Results are:

Link	Diameter [m]	Length [m]	Beamwidth [deg]
D/L	0.0347	0.0284	142.92
U/L	12.23	-	0.755

These results are in line with the datasheet data of the real hardware.

⁸In that case low free space losses allow us to trade a little bit higher power budget from TTMC gaining an easier/lighter ADCS design.

Losses In order to determine the link budget, losses and noises must be calculated. Free space losses in particular can be computed as:

$$L_s = -147.55 + 20\log(S_{worst}) + 20\log(f) \rightarrow L_{s,D/L} = 167.92\text{ dB} \quad L_{s,U/L} = 167.52\text{ dB}$$

To count all other types of losses (e.g cable, pointing, polarization, atmospheric...) and the realization margin (MAR-COM-060), $L_{add} = 5\text{ dB}$ has to be considered for all links design.

Noise In order to compute the equivalent noise temperature T_s some assumptions are made:

- Earth-facing links (as D/L) will suffer mostly the thermodynamic temperature of the planet itself $T_{ant,Main} = 290\text{ K}$;
- The Sky-facing link (as U/L) will suffer from cosmic rays mostly with $T_{ant,Kiruna} = 10\text{ K}$.
- The receiver noise temperatures are $T_{rec,Kiruna} = 93\text{ K}$ (from ESA's documents) and $T_{rec,Main} = 580\text{ K}$ (assumption based on literature);

From these assumptions it is possible to obtain:

$$T_{D/L} = T_{rx,Kiruna} + T_{tx,MANGO} = 283\text{ K} \quad T_{U/L} = T_{tx,Kiruna} + T_{rx,MANGO} = 590\text{ K}$$

Link budget E_b/N_0 it can be finally computed with the following expression:

$$\frac{E_b}{N_0} = P_t + G_t + G_r - L_s - L_{add} + 228.6 - 10\log(T_s) - 10\log(R)$$

Using the procedure seen above we get the following link budgets:

D/L	22.94 dB
U/L	64.61 dB

7.4.3 Inter-Satellite Link (ISL)

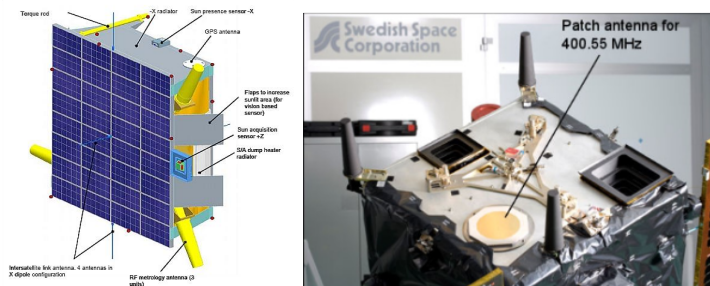


Figure 26: ISL link architecture

The Inter-Satellite Link (ISL) allows Tango to communicate with the ground through Mango. It works in UHF-band to minimize Tango power budget and it is designed with:

- Dual-Dipole configuration (4 antennas) on Tango (Target) to achieve full-spherical coverage and avoid additional pointing budget;
- A patch antenna (great choice from a configuration point of view) on Mango (Main) along rendezvous direction since nominally it's the only one of interest;

Data are:

R [kbit/s]	P_t [dBm]	G_t [dB]	G_r [dB]	S_{worst} [km]	f [MHz]
19	10	3.1	1.64	10	450

Then the antenna dimensions can be calculated:

L (Tango,Dipole) [m]	D (Mango,Patch) [m]
0.33	0.16

Assuming a worst-case scenario where the link is Earth facing and assuming a typical receiver, the noise temperature is obtained:

$$T_s = T_{ant} + T_{rec} = 290K + 580K = 870K$$

So losses and link budget are:

L_s [dB]	Eb/N0 [dB]
105.51	30.64

7.4.4 Radio frequency Link

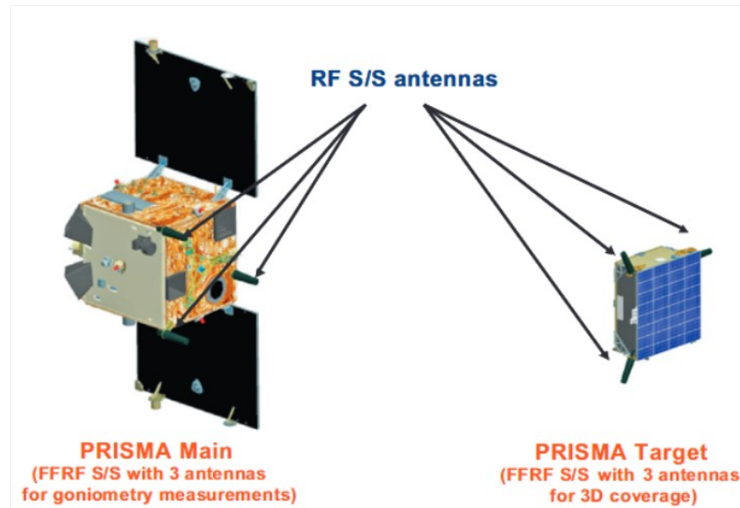


Figure 27: RF link architecture

Both spacecrafts have as a payload an RF link: the main has both Tx/Rx capabilities, while the target only Tx. The terminal in fact works in a dual frequency S-band: one for telemetry (Tango can send telemetry to Mango as ISL redundancy) and one for ranging purposes. Since only the first one carries data, it will be the only one analyzed. In particular, the architecture of this link is composed by:

- Three Helix antennas (number constrained by triangulation capabilities) on Mango along rendezvous direction (nominally towards the target);
- Three Helix antennas on Tango to reach full spatial coverage and reduce pointing budget.

The properties of the system in both directions are the following:

R [kbit/s]	P_t [dBm]	G_t [dB]	G_r [dB]	S_{worst} [km]	f [MHz]
12	20	4	4	30	2275

Using the same assumptions used for ISL with respect to the noise temperature, the following results are achieved:

L_S [dB]	E_b/N_0 [dB]	D [m]	L [m]	Beamwidth [deg]
105.51	45.22	0.033	0.046	107.17

7.5 Link margins

In this mission, a Convolutional coding ($k/n=2$, $K=7$) has been considered with a QPSK modulation strategy ⁹. With the assumed BER of 10^{-6} , it is possible to retrieve the ideal E_b/N_0 ratio from theory (Figure 41).

$$\frac{E_b}{N_{0ideal}} \approx 11dB$$

Comparing this result with link budgets previously found and computing the margins by considering also 3 dB from MAR-COM-030 by ESA guidelines:

Link type	Link budget margin [dB]
Downlink (S-Band, TM/Science)	9.94
Uplink (S-Band, TC/Navigation)	51.62
ISL (UHF)	17.64
RF (S-Band)	9.28

All margins are positive so the sizing is correct¹⁰. For sake of completeness are reported also the margin on SNR (Signal Noise Ratio) ¹¹.

⁹As a consequence, the data rate R at the end of encoding and modulation phases will be unchanged ($\alpha_{enc} = \alpha_{mod} = 2$)

¹⁰In reality these values are still slightly high: it's necessary to change some data (e.g. powers, gains, dimensions...) and iterate until they all become more or less 4-6 dB each

¹¹Assumptions are: Datarate R equal to bandwidth B, modulation index $\beta_{mod} = 60$ deg, $SNR_{min,Kiruna} = 10$ dB and 3 dB of SNR margin.

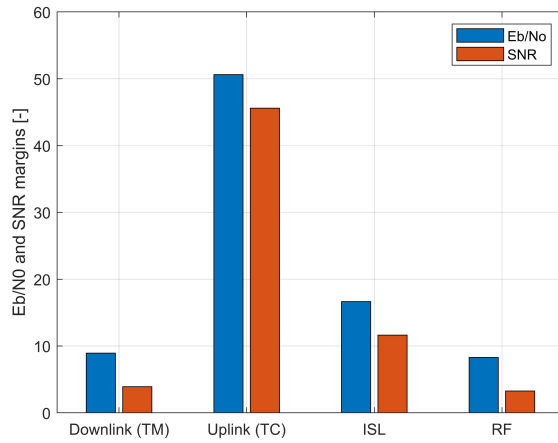


Figure 28: Link margins chart

7.6 Amplifier selection

In order to compute link margins, transmitted power values were taken from PRISMA datasheets, but it's important to point out that these power budgets come from:

$$P_{Tx} = P_{Amp,Output} = \eta_{Amp} P_{Amp,Input}$$

Since both spacecrafts work with very low power values, the optimal amplifier choice is a Solid State Amplifier (SSA) for each link. The principal advantages obtained with respect to a Traveling Wave Tube one (TWTA) are the following: lower cost, more compact and lighter, higher output linearity, and lower voltage required. The biggest disadvantage instead is a large amount of heat generated, which shall be considered in the TCS analysis. For them it can be considered an average efficiency of $\eta_{Amp} = 3\%$ (Figure 41).

7.7 Mass and power budget

From off-the-shelf component datasheets:

	Mass [gr]	Power [W]
Multiplexer (both)	1x200	1x3
UHF Trans-receiver (both)	90	2
S-Band Trans-receiver (both)	200	6.5
UHF Dipole Antenna (Tango)	4x10	4x2.5
UHF Patch Antenna (Mango)	1x50	1x2
RF Helix Antenna (both)	3x235	3x1
S-Band Helix antenna (Mango)	2x140	2x10

These values are fine: for instance, considering the Main to Earth downlink with $P_{tx} = 0.5 W$ and the above reported $P_{trans,S-Band} = 7.4W$, is found that $\eta_{amp} = 6.75\%$, which is in line with SSA literature.

Final results are obtained by considering for the mass budget the sum of all components while for the power budget the highest power demanding antenna and relative components. In the following table the entire budgets are shown:

	Mass budget [Kg]	Power budget [W]
Mango (Main)	2.3	38.4 (using S-Band Helix Antenna)
Tango (Target)	1.6	19.5 (using UHF Dipole Antenna)

Considering a $M_{dry} = 128 \text{ Kg}$ (real from PRISMA datasheets) and taking a reference chart from literature (Figure 38), is verified that $M_{TTMC} \sim 5 \text{ Kg}$, so the computations made are fine.

8 Attitude Determination and Control Subsystem (ADCS)

8.1 Generalities and requirements

The two ADCS s/s of the PRISMA mission are directly involved in successfully carrying out its experiment. Since the mission is a GNC manoeuvres/sensors on-orbit test-bed, this specific subsystem is a crucial driver: it needed a lot of redundancies (cold ones) to ensure the success of the mission.

Mango requirements Taking literature as reference:

Main ADCS requirements
<ul style="list-style-type: none"> • Mango ADCS shall be able to de-tumble from rates up to 2 deg/s in less than 5 minutes; • Mango ADCS shall have a safe sun mode able to point solar arrays toward sun direction (± 20 deg range) with an accuracy of < 5 deg; • Mango ADCS shall have a safe celestial mode able to point solar arrays towards Sun direction (± 20 deg range) with an accuracy < 1 deg; • Mango ADCS shall have a normal mode able to point GPS antenna towards zenith direction (± 20 deg range) with an accuracy of < 1 deg; • Mango ADCS shall have a tracking mode able to point VBS/FFRF/ISL toward the target direction (± 20 deg range) with an accuracy of < 1 deg; • Mango ADCS shall be able to perform each slew maneuver required by GNC experiments, so in the worst case 45 deg in less than 2 min; • Mango ADCS shall have an exclusion zone on the sun for optics field of view; • Mango ADCS shall ensure 3-axis stabilization during thrusting phases;

Tango requirements From the literature can be summarized as:

Target ADCS requirements
<ul style="list-style-type: none"> • Tango ADCS shall be able to de-tumble from rates up to 2 deg/s in less than 15 minutes; • Tango ADCS shall be able to slew from any attitude to sun direction in less than 30 minutes; • Tango ADCS shall have a safe mode able to point solar arrays toward Sun direction (± 20 deg range) with an accuracy of <5 deg; • Tango ADCS shall have a normal mode able to point GPS toward zenith direction (± 20 deg range) with an accuracy of <5 deg; • Tango ADCS shall be able to mimic a non-cooperative tumbling mode.

Other s/s requirements ADCS s/s is influenced by EPS, TTMTTC and TCS pointing requirements. Nevertheless, it's also linked with OBDH design: in order to perform correctly all the experiments needed for instance to manage relative navigation sensors (GPS, FFRF, VBS), execute control algorithms, validate commanded maneuvers, store attitude data, and so on.

8.2 Disturbance torques analysis

In order to characterize the actuators, first, the disturbance torques acting upon both spacecrafts have to be computed. Internal disturbances at this stage of sizing are neglected, whereas for external ones some simplifications are made: the major inertia axis has been computed as $I = 0.01M^{5/3}$, circular orbit of $h = 720$ km and torques are considered static.

Gravity gradient This disturbance has been computed in the case of maximum attitude asymmetry $\theta = 45^\circ$:

$$T_{gg} = \frac{3\mu}{2R^3} |I_{max} - I_{min}| \sin(2\theta_Y)$$

where R is the radius of the position vector of the satellite and μ is the planetary constant of the Earth.

Aerodynamic drag To model this contribution the following formula is used:

$$T_{drag} = \frac{1}{2}\rho C_d A V^2 (c_p - c_g)$$

In particular, C_d is considered equal to 2.5 and ρ is taken from ISA standard atmosphere tables.

Solar radiation pressure The SRP torque has been modeled through the following relations:

$$T_{srp} = p_{srp} (c_{ps} - c_g) (1 + q)$$

where the reflectance factor q is assumed to be equal to 0.5 and the equivalent solar radiation pressure p_{srp} is given by the ratio between the solar irradiance at 1 AU and the speed of light.

Magnetic torque

$$T_{magn} = D_{s/c} B_{polar} = D_{s/c} \frac{2B_0 R_0}{r^3}$$

The residual dipole is assumed as 10^{-3} Am^2 as suggested by NASA guidelines (NASA SP-8018).

Torque [Nm]	Mango	Tango
SRP	$2.8642 \cdot 10^{-6}$	$3.856 \cdot 10^{-7}$
Atmospheric Drag	$4.107 \cdot 10^{-6}$	$7.291 \cdot 10^{-8}$
Gravity Gradient	$3.353 \cdot 10^{-5}$	$3.920 \cdot 10^{-6}$
Magnetic Torque	$1.109 \cdot 10^{-21}$	$1.109 \cdot 10^{-21}$

Analysis of results Moreover, since the PRISMA mission has a Sun-Synchronous orbit and nominally Mango and Tango are pointing nadir direction, the only cyclic external disturbance under these conditions is the Magnetic one.

8.3 Architecture and sizing

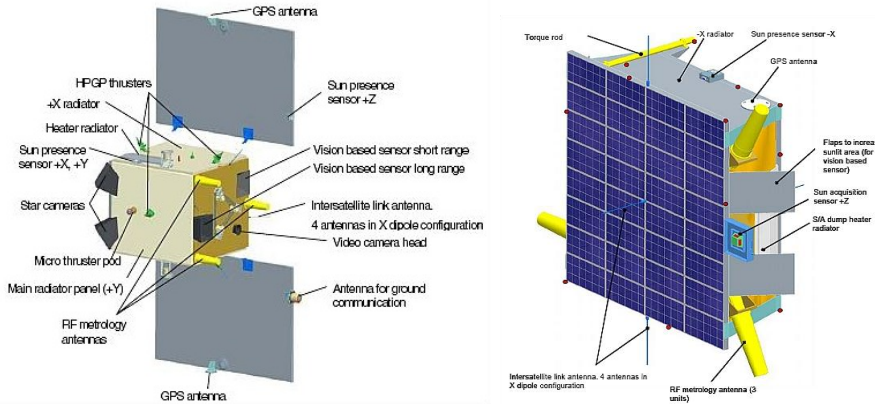


Figure 29: Mango/Tango sensors architectures

8.3.1 Mango (Main) ADCS

Sensors Mango ADCS sensors are designed as follows:

- One fine sun sensor (20 deg FoV) on solar panels (sun tracking) and two 3-axis magnetometers to satisfy safe sun mode (two vectors needed) and to be redundant ($< 5 \text{ deg}$ of accuracy);

- Five gyros and two star-trackers for safe celestial and normal mode and to be redundant ($< 1 \text{ deg}$ accuracy);
- Two Vision-Based Sensors (P/L) along rendezvous direction for relative navigation mode;
- Six sun presence sensors (one for each surface) for a cheap and full sun position estimation.

To summarize, in order to estimate Mango attitude, two complete, independent and redundant sets of sensors with different levels of accuracy (by requirements) are needed to satisfy all Mango attitude modes. Sun sensors and magnetometers are very simple, reliable and with low power consumption, gyros and star trackers instead are more delicate (gyros need a frequent re-calibration, and star trackers should avoid sun inside their FoV) and heavy under the power budget point of view, but they give higher accuracy (needed for Target and GPS pointing).

Moreover, in order to provide also Target attitude/position information during relative navigation mode, a VBS system is installed on Mango rendezvous direction. This sensor, however, isn't directly part of the platform design, it's a payload and it's used during specific GNC experiments.

Actuators Mango ADCS has the following actuators:

- Four Reaction Wheels in tetrahedral configuration for redundancy to ensure very fine 3-axis control and fast slew maneuvers;
- Three magnetic rods for angular momentum management (in LEO taking advantage of \vec{B}_{earth} avoid propellant usage);

Sizing Knowing already external disturbance torques, the requested torque for attitude maneuvers has to be computed:

$$T_{\text{det}} = \frac{I\omega}{\Delta t} = 0.0047 \text{ Nm} \quad T_{\text{slew}} = \frac{4I\omega}{\Delta t^2} = 0.0087 \text{ Nm}$$

The gravity gradient was the most important disturbance but these torques are three orders of magnitude higher. The reaction wheels (RWs), in order to have enough control authority, should have:

$$T_{\text{RW}} = 2T_{\text{max}} = 2T_{\text{slew}} = 0.0147 \text{ Nm}$$

The angular momentum stored by the RWs in each orbit should be now evaluated:

$$H_{\text{stor}} = \Delta T_{\text{orb}} \frac{T_{\text{gg}}}{4} 0.707 = 0.035 \frac{\text{kgm}^2}{\text{s}}$$

In order to have a momentum management action more or less every two days ($\sim 30 \text{ orbits}$), a small size off-the-shelf reaction wheel with $H_{\text{max}} = 1 \text{ Nms}$ can be taken.

Assuming 60 min for each de-saturation action, the magnetic dipole needed by magnetic rods is:

$$D = \frac{H_{stor}}{B_0 \Delta t_{desat}} = 8.96 \text{ Am}^2$$

8.3.2 Tango (Target) ADCS

Sensors Tango has on board the following sensors:

- One sun sensor (± 25 deg FoV) on solar panels (sun tracking) and one 3-axis magnetometer to satisfy safe sun mode (< 5 deg of accuracy);
- Six sun presence sensors (one on each side) as before.

Tango only needs these two sensors to compute its attitude, it doesn't need another type of sensor because it rarely enters an eclipse phase and it doesn't need a good pointing accuracy, thus there's no need for a star tracker. Sun presence sensors are useful for not nominal conditions where the Sun is outside the FOV of the fine sun sensor.

Actuators Tango has on board the following actuators:

- Magnetic rods for cheap, reliable, and coarse control.

Tango has no ΔV capability and it doesn't require a good pointing accuracy. Reaction wheels would require at least a second actuator due to saturation and thus would require a high mass and power budget.

Sizing Tango highest needed torque is the one for the de-tumbling after the Mango release. Our reverse engineering workflow and results are:

$$T_{det} = \frac{I_{max}\omega}{\Delta t} \rightarrow D = \frac{T_{det}}{B_0} \text{ with } B_{polar} = \frac{2M_0}{R_{orb}^3}$$

T[Nm]	D[Am ²]	D _{max,real} [Am ²]
$6.69 \cdot 10^{-5}$	2.94	2.5

Considering the approximations used, this result is in line with the real mission.

8.4 Mass and power budgets

From off-the-shelf component datasheets, it is possible to report the following components for Mango:

	Mass [g]	Power [W]
Star tracker	2x425	2x1.9
Magnetometers	2x85	2x0.75
Fine Sun Sensor	300	1
Sun Presence Sensor	6x45	6x0.02
Gyros	5x55	5x1.5
Reaction Wheels	4x226	4x0.9
Magnetic Rods	3x550	3x0.7
VBS	2x350	2x0.7

And for Tango, considering every component as cold redundant:

	Mass [g]	Power [W]
Fine Sun Sensor	2x300	1
Magnetometer	2x85	0.75
Sun Presence Sensor	2x6x45	6x0.02
Magnetic Rods	2x3x250	3x0.5

Final budgets are:

	Mass budget [kg]	Power budget [W]
Mango (Safe-Sun mode)	6.6	9.8
Mango (Safe-Celestial mode)	=	16.6
Tango	3.7	4.4

Notice that, for Mango, the power budget difference depending on the set of sensors used is highlighted: star trackers/gyros use much more power than sun sensors/magnetometers.

9 Electrical Powers Subsystem (EPS)

9.1 Generalities and requirements

Each Mango/Tango subsystem needs the power to work and so it's necessary to analyze both Electrical Power Subsystems. It does not only provide power generation, but also storage, regulation and distribution. Requirements are:

Main/Target EPS requirements

- Main/Target EPS shall be able to provide a power of TBD W at 28V for the spacecraft s/s and p/l during all the mission;
- Main/Target batteries shall cover the power needs during eclipses (20 mins only during an eclipse season) and safe mode conditions;
- Main/Target solar arrays shall be sized according to operational life and debris impact, radiations and atomic oxygen interaction;
- Main/Target EPS shall have an operating lifetime of at least 1 year;
- Main/Target EPS shall provide telemetry and command for status and health;
- Main/Target EPS regulation and control shall respect each loads requirements;

9.2 Architecture



Figure 30: PRISMA spacecrafts solar panels

Power generation As a primary energy source, since the spacecraft is in a LEO orbit, solar panels are a straightforward choice for both spacecrafts. Their sizing will be mostly driven by the power budget and, moreover, notice that on Mango solar panels are mounted on wings to increase exposed area and reduce heat problems, while on Tango are body mounted to avoid a double packed/unpacked configuration.

Power storage Despite PRISMA orbit maintaining very few and short eclipses, batteries are needed mostly for reliability. Due to their very high energy and power density Li-ion batteries nowadays are the optimal choice. Mango uses two batteries for redundancy and Tango one.

Power distribution, regulation and control Due to our spacecraft sizes (power budget for sure $< 2 \text{ kW}$) bus voltage will be $\Delta V_{bus} = 28 \text{ V}$. The mission is very short

and so Mango/Tango will probably adopt a Peak Power Tracking (PPT, non-dissipative and active device with $X_e = 0.6 / X_d = 0.8$) primary source control; instead for the bus control a quasi-regulated strategy, due to the almost non-existent eclipse condition, is the best choice.

Available data and considerations From the literature it is possible to retrieve the following data:

	A_{sp} [m ²]	P_{sp} [W]	C_{batt} [Wh]
Mango(Main)	2x1	300	3x100
Tango(Target)	0.5	90	2x45

Moreover notice that EPS design influences TCS (heat generation), OBDH (health and status), ADCS (arrays pointing) and STR (arrays position).

9.3 Sizing

9.3.1 Power breakdown

Before starting with sizing, since so far not all Mango/Tango subsystems have been analyzed, in order to try to have a reference of the total worst-case power budget of both spacecrafts, the group has analyzed both the calculations already made and literature. Proceeding using as reference ADCS and TTMC power budget:

ADCS	P budget [W]	TTMTC	P budget [W]
Mango (Main)	9.8	Mango (Main)	38.4
Tango (Target)	4.4	Tango (Target)	19.5

From theory is available statistical data in a table form (Figure 39) allowing to obtain with a reverse engineering approach the following results:

	Mango(Main)	Tango(Target)
P_{total} [W]	128-150	40-59

9.3.2 Power storage

In order to make some computations, Li-ion batteries' efficiency is assumed from the literature. Chosen Depth Of Discharge from charts (Figure 42) and the longest eclipse period: $\eta_{batt} = 0.9$, $DoD = 80\%$ (very few C/D cycles) and $T_{max,eclips} \approx 20 \text{ min}$. Now it can be computed the power available from batteries (excluding redundant ones) during eclipses knowing their capacities:

$$P_e = \frac{C_r DDoD \eta_{batt}}{T_e} \rightarrow P_{e,main} = 189 \text{ W} \quad P_{e,target} = 85.35 \text{ W}$$

From literature it is confirmed that batteries are sized to keep everything switched on, therefore these calculations are plausible. It is possible to compute even the available power during a possible safe mode to use at least TTMC and OBDH s/s, so considering the entire orbital period as discharge and a 100% DoD:

$$P_{safe,main} = 49.09 \text{ W} \quad P_{safe,target} = 42.03 \text{ W}$$

These results are both expected since from the previous power budget breakdown these are in the order of magnitude of the TTMTTC power budget.

9.3.3 Power generation

Main/Target use Gallium/Arsenide (GaAs, multi-junction type) solar arrays. Some data useful for the computations are:

	I_d [-]	d [-]	η_{sa} [-]
Ga/As SA	0.77	0.0375	0.18

At least one year of operating life is requested and the worst-case Solar Aspect Angle can be taken as $\alpha_{SSA} = 23.5 \text{ deg}$ (obliquity angle). So now, using the following formulas:

$$P_{SA} = A_{sa} P_{EOL} = A_{sa} P_{BOL} (1 - d)^{years} = A_{sa} \eta_{sa} P_{sun} I_d \cos \alpha_{SSA} (1 - d)^{years}$$

The power produced by the solar panels, knowing the exposed area, is obtained:

$$P_{SA,main} = 332.27 \text{ W} \quad P_{SA,target} = 83.06 \text{ W}$$

These results are equal to the original ones from PRISMA mission literature.

Knowing the power generated by each solar array, it can be verified the highest power budget (among all modes) of both spacecrafts, hence the value driving the EPS design:

$$P_d = \left(P_{sa} T_d - \frac{P_e T_e}{X_e} \right) \frac{X_d}{T_d}$$

	Mango(Main)	Tango(Target)
P_d [W]	202.02	37.74

Taking these results and adding from MAR-PWR-040 a 20% power margin, it can be verified their correctness by reporting again the statistical reference values from the power breakdown:

	Mango(Main)	Tango(Target)
$P_{d,nomargins}$ [W]	161.61	30.19
$P_{d,statistical}$ [W]	150	40

9.3.4 Bus voltage

Now, the number of solar cells and batteries in series to reach the nominal voltage value of 28V for both Mango and Tango can be computed.

- Assuming that each GaAs solar cell has a $V_{cell} = 2.6 \text{ V}$ result is:

$$N_{ser,cell} = \text{ceil} \left(\frac{V_{s/c}}{V_{cell}} \right) = 11$$

- Assuming that each Li-Ion battery has a $V_{cell} = 3.6 \text{ V}$ result is:

$$N_{ser,cell} = \text{ceil} \left(\frac{V_{s/c}}{V_{cell}} \right) = 8$$

Therefore during sunlight, the voltage will be constant at 28.6 V (without considering lock-ups), while during eclipses the batteries guarantee nominally (far from complete discharge) a voltage of 28.8 V.

9.4 Mass budget

Batteries and solar arrays sizing allows proceeding with the computation of Main/Target EPS mass budgets. The formulas used come from SMAD and they are: batteries mass $m_{batt} = \frac{C_r}{E_d}$, solar arrays mass $m_{sa} = 0.04P$, PCU mass $m_{CPU} = 0.02P$, regulators/converters mass $m_{reg,conv} = 0.025P$, wiring mass: $m_{wir} = 0.04m_{dry}$. Results compared to literature (20% dry mass) are:

	Mango(Main)	Tango(Target)
$M \text{ [Kg]}$	31.42	7.31
$M_{expected} \text{ [Kg]}$	29	9

10 Thermal Control Subsystem (TCS)

10.1 Generalities and requirements

The Thermal Control Subsystem shall maintain the spacecraft within its correct temperature operational values under each mode and phase.

Main/Target TCS requirements

- Mango (Main) and Tango (Target) batteries temperature shall be within $[0;+40] \text{ } ^\circ\text{C}$;
- Mango (Main) and Tango (Target) solar arrays shall be within $[-165;+130] \text{ } ^\circ\text{C}$;
- Mango (Main) optics and Mango/Tango (Target) electric components shall have thermal stability of TBD $\text{ } ^\circ\text{C}/\text{s}$ and a maximum gradient of TBD $\text{ } ^\circ\text{C}/\text{mm}$.

10.2 Architecture and sizing

10.2.1 Mango (Main) single node

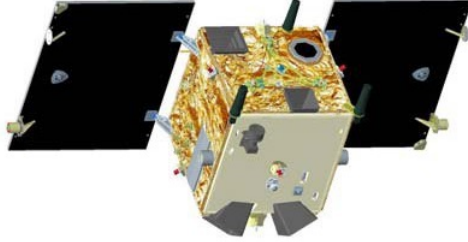


Figure 31: Mango (Main) external coatings

Mango possess five sides coated with MLI (layers of Al-Kap, great to decouple s/c-environment) with overall $\alpha = 0.01$ and $\varepsilon = 0.03$ (Figure 43) and the entirely shadowed one (-pitch), used as radiator, made of Anodized Aluminum (typical solar reflector) with $\varepsilon_{rad} = 0.7$. Design temperature range is driven mostly by Li-ion batteries; taking into account requirements and MAR-TCS-010 it results $\Delta T = [+15; +25]^{\circ}\text{C}$.

Starting from the hot case, considering as internal power the entire power budget (worst case) and all the s/c covered with MLI (in order to verify the need for a radiator) the following results are obtained ¹²:

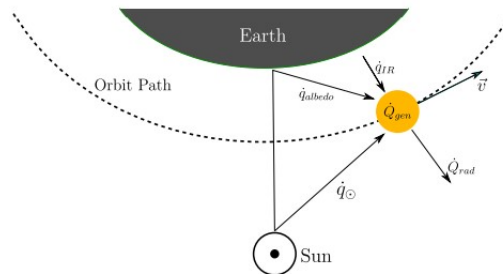


Figure 32: Heat transfer model diagram

$$\begin{aligned} A_{tot}\varepsilon\sigma T_{max}^4 &= Q_{sun} + Q_{IR} + Q_{alb} + Q_{int} = \\ &= A_{sun}\alpha \cos \theta_{sun} q_0 R_{s/c}^2 + A_{pl} \cos \theta_{pl} \sigma \varepsilon T_{pl}^4 \frac{R_{pl}^2}{R_{orb}^2} + A_{pl}\alpha \cos \theta_{pl} q_0 a \frac{R_{pl}^2}{R_{orb}^2} + Q_{int} \end{aligned}$$

Q_{sun} [W]	Q_{IR} [W]	Q_{alb} [W]	Q_{int} [W]	T_{hot} [$^{\circ}\text{C}$]
14.22	5.14	4.02	150	96.97

¹²In the computation of the albedo contribution 'a' is an averaged term, in more refined computations the beta-angle β (almost 90° here) shall be taken into account.

A radiator is clearly needed here to decrease the steady-state hot temperature. In order to respect the requirements, it is imposed the maximum temperature and it is computed the needed area of the radiator (considered a structural panel) with the following equation:

$$A_{rad}(\varepsilon_{rad} - \varepsilon)\sigma T_{max}^4 = Q_{sun} + Q_{IR} + Q_{alb} + Q_{int} - A_{tot}\varepsilon\sigma T_{max}^4$$

All power contributions remain the same and the radiator area results in $A_{rad} = 0.36 m^2$; it's a great result since in reality this surface is $A_{real} = 0.64 m^2$. The last passage is to verify with that configuration also the cold mode:

$$(\varepsilon A_{tot} + (\varepsilon_{rad} - \varepsilon) A_{rad}) \sigma T_{max}^4 = Q_{IR} + Q_{int}$$

The result is $T_{cold} = 16.83 {}^\circ C$ which is fine, given the required range.

10.2.2 Tango (Target) single node

Tango instead has been modeled in two nodes: one for the platform and one for the solar array. Emissivity and absorptivity coefficients (Figure 43) are:

	α	ε
Solar array	0.8	0.82
White paint	0.3	0.8

Being in an SSO orbit a solar reflecting coating as a white paint is a good choice. The link between the two nodes is modeled as a polymeric insulant panel with $k_{lin} = 0.1$ and $t = 5 mm$. The platform has a sharper operational temperature range, it is better to keep as much heat as possible on the solar panel. With these considerations and proceeding with the hot case computations, the results are:

$$\begin{cases} A_{plat}\varepsilon_{plat}\sigma T_{plat}^4 + k_{ins}\frac{S_{ins}}{t_{ins}}(T_{plat} - T_{sp}) = Q_{IR} + Q_{alb} + Q_{int,plat} & Platform \\ A_{plat}\varepsilon_{sp}\sigma T_{sp}^4 + k_{ins}\frac{S_{ins}}{t_{ins}}(T_{sp} - T_{plat}) = Q_{sun} + Q_{int,sp} & Solar panel \end{cases}$$

Q_{sun} [W]	Q_{IR} [W]	Q_{alb} [W]	$Q_{int,sa}$ [W]	$Q_{int,plat}$ [W]	$T_{sa,hot}$ ${}^\circ C$	$T_{plat,hot}$ ${}^\circ C$
700.16	31.75	27.81	59	218.56	46.66	16.23

Considering the requirements of the platform, again driven by the presence of Li-ion batteries, the results are acceptable. For the cold case the following results are obtained:

$$T_{sa,cold} = -101.89 {}^\circ C \quad T_{s/c,cold} = -99.90 {}^\circ C$$

Solar array temperature might be fine, while platform temperature is certainly wrong. Since there are very few eclipses of 20 minutes maximum, Tango never reaches such a low steady-state temperature. Therefore the steady-state cold case is not accurate, it is needed more accurate models. In fact, taking into account Fourier's law and integrating it is obtained that Tango in 20 minutes loses approximately only $3 {}^\circ C$:

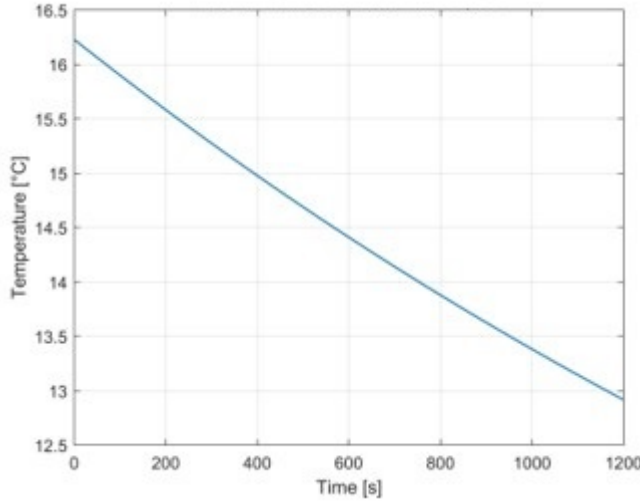


Figure 33: Tango (Target) temperature transient

11 Structural Subsystem (STR)

11.1 Generalities and requirements

Mango (Main) and Tango (Target) structures shall transmit loads to the base of the satellites supporting appropriately both spacecrafts during their life (e.g. launch, maneuvers,...), maintain the required configuration, and provide environmental protection, thermal and electrical paths. Requirements for the structural design are:

Main/Target STR requirements

- Main/Target structure shall be compatible with launch static/dynamic loads and separation event shocks;
- Main/Target structure shall be compatible with steady-state thruster acceleration and transient loads during attitude maneuvers;
- Main/Target structure shall be sized taking into account UV, TID/DDD, AO degradation during the entire mission lifetime;
- Main/Target structure shall be manufactured at SSC HQ in Solna (Sweden);
- Main solar arrays deployment shall be tested on-ground with a specific test-bed;
- Main/Target structures coupled shall fit inside launcher fairing envelope.

11.2 Mango/Tango configurations

Knowing both spacecrafts components and subsystems, they can be put together by choosing a specific configuration. Guidelines are:

- Mango configuration:
 1. P/L should be positioned first: HPGP/MEMS aligned with the CoM, VBS/F-FRF/ILS along rendezvous direction;
 2. All propellant tanks as near as possible to the CoM and symmetrical;

3. Hydrazine Thrusters along identified directions by ADCS engineer and maximize their levers;
4. GPS and S-Band antennas along zenith/nadir direction for better pointing;
5. Transmitters near antennas to reduce cable length and distribute heat sources better;
6. Radiator surface towards shadowed side;
7. Sun sensor directed towards the Sun and Magnetometers, RWs, and Magnetic-Rods on a stiff and thermally stable panel;
8. Star Tracker cameras on the eclipsed surface (avoid Sun contact) and far from thrusters contamination.

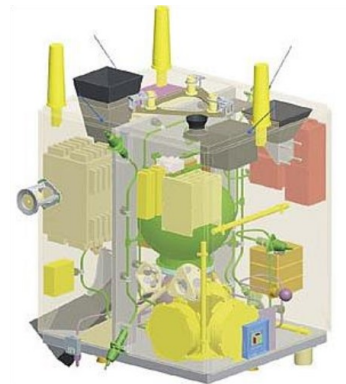


Figure 34: Mango (Main) configuration

- Tango configuration:
 1. FFRF/ILS placed to reach spherical coverage;
 2. GPS antennas along zenith direction for better pointing;
 3. Transmitters near antennas to reduce cable length and distribute heat sources better;
 4. OBDH components and batteries far from solar arrays and closer among them to need fewer cables and dissipate heat better.

Notice that Mango needs two configurations (packed and unpacked) in order to fit under DNEPR fairing. Chosen both configurations and computed the needed dimensions, it can be cross-checked that Mango/Tango packed with Picard can be easily fitted in. Spacecrafts are 1.6x0.8x0.8 m and instead the available space inside the fairing is approximately 3.1x1.9x1.9 m.

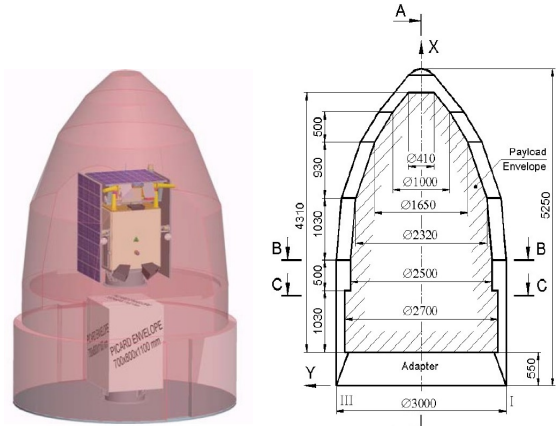


Figure 35: Configuration at launch and fairing envelope

11.3 Sizing

The launch environment is the most critical for the structure and so it's the one considered for the first sizing. Moreover, Mango and Tango structures are considered as a unique hollow parallelepiped of Aluminum¹³ ($\sigma_{Al} = 257 MPa$, $E_{Al} = 70 GPa$) with dimensions 800x800x1600 mm (a=b=800 mm, L=1600 mm) and a wet mass of 190 kg (MAR-STR-030). Load factors and fundamental frequencies were taken directly from the DNEPR manual as follows (frequencies will be increased by a 15% margin due to MAR-STR-020):

$$\begin{aligned} n_{ax} &= 7.5 \text{ g} & n_{mom} &= 3 \text{ g} \\ f_{ax} &= 20 \text{ Hz} & f_{lat} &= 10 \text{ Hz} \end{aligned}$$

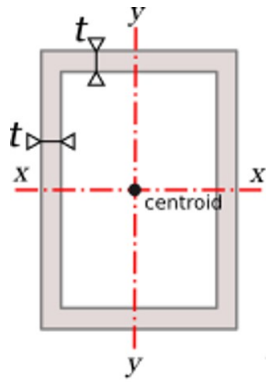


Figure 36: Structure internal geometry

The object of the sizing will be panel thickness. The buckling constraint will be the most critical, so firstly, it must be computed the minimum panels' thicknesses to satisfy strength and stiffness constraints. The static equivalent load is:

¹³Compared with a Composite Material is heavier, but cheaper and with an easier design.

$$P_{eq} = n_{ax}m + \frac{4n_{mom}m}{b} = 51.7 \text{ kN}$$

Then, imposing a-priori $MS_{strength} = 1$ and $fos_{\sigma_{app}} = 2$ (ECSS-E-ST-32-10C) for robustness, thickness for strength resulted combining some formulas:

$$A(t) = (MS + 1) f \frac{P_{eq}}{\sigma_{Al}} \rightarrow t_{min,str} = 0.39 \text{ mm}$$

Instead, the thicknesses to satisfy minimum axial and lateral resonance frequencies (Figure 44, in this case, modeled as a beam) are:

$$f_{ax} = 0.25 \sqrt{\frac{AE_{Al}}{mL}} \quad f_{lat} = 0.56 \sqrt{\frac{E_{Al}I}{mL^3}}$$

$$t_{min,ax} = 0.011 \text{ mm} \quad t_{min,lat} = 0.027 \text{ mm}$$

Minimum thicknesses for strength and stiffness impose a lower bound. At this point, the idea is to increase the thickness until the buckling margin of safety becomes positive. The formula used ($k=5.64$, C-SS panel), starting from MS_{buck} definition and making some substitution, is:

$$MS_{buck}(t) = \frac{k\pi^2 E_{Al}}{12(1-\nu^2)} \left(\frac{t}{b}\right)^2 \frac{4bt}{P_{eq}} - 1$$

Notice that each thickness value also applied stress changes. Result is:

$$t_{min,buck} = 3.31 \text{ mm}$$

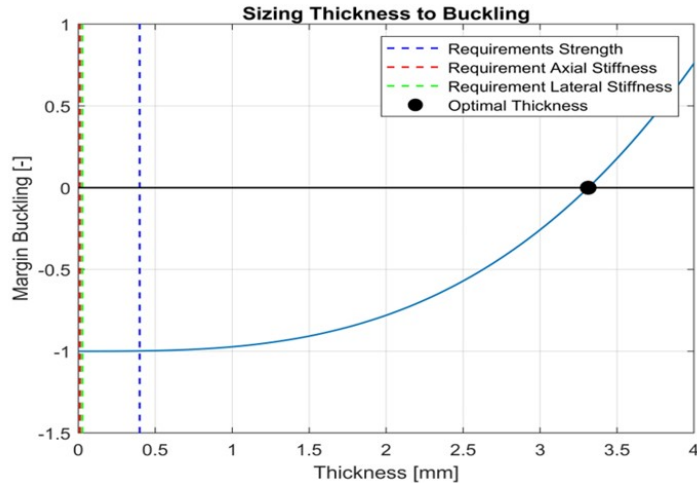


Figure 37: Thickness versus margin on buckling condition

12 Bibliography

- [1] Larson, W J, and Wertz, J R. Space Mission Analysis and Design. United States: N. p., 1992.
- [2] CDF Standard Margin Philosophy , Issue 1 Revision 2, TEC-SYE, OPS-GFA, SCI-FMA, TEC-E, TECM, TEC-S, 2017.
- [3] PRISMA (Prototype) - eoPortal Directory - Satellite Missions." PRISMA (Prototype) - eoPortal Directory - Satellite Missions, earth.esa.int, <https://earth.esa.int/web/eoportal/satellite-missions/p/prisma-prototype>. Accessed 7 Aug. 2022.
- [4] Dnepr User Guide - [PDF Document]." Fdocuments.Net, [fdocuments.net](https://fdocuments.net/document/dnepr-user-guide.html), <https://fdocuments.net/document/dnepr-user-guide.html>. Accessed 7 Aug. 2022.
- [5] ESTRACK Operations Manual, Volume 2, Network Control Procedures, DTOS-ESTR-OPS-OM-1001-TOS-ONF, Issue 7, Revision 0, 2000.
- [6] Bodin, P. et al., "The PRISMA Formation Flying demonstrator. Overview and Conclusions from the main mission", Proceedings of the 35th annual AAS Guidance and Control Conference, February, Breckenridge, Colorado, 2012.
- [7] Staffan Persson and Björn Jacobsson. "PRISMA Swedish In-orbit Testbed for Rendezvous and Formation Flying," AIAA 2006-D1.2.02. 57th International Astronautical Congress, 2006.
- [8] Eberhard Gill, Simone D'Amico, and Oliver Montenbruck, "Autonomous Formation Flying for the PRISMA Mission", Journal of Spacecraft and Rockets, 2007.
- [9] S. Persson, B. Jakobsson and E. Gill, "PRISMA, Demonstration Mission for Advanced Rendezvous and, Formation Flying Technologies and Sensors," Number 05-B56B07, 56th International Astronautical Congress, Fukuoka, Japan, International Astronautical Congress, 2005.
- [10] Damico, S. et al., "Navigation of Formation Flying Spacecraft using GPS: The PRISMA Technology Demonstration", 22–25 September, ION-GNSS 2009, Savannah, USA, 2009.
- [11] Delpech, M. et al., "Preliminary results of the vision based rendezvous and formation flying results performed during the PRISMA extended mission", DyCoss 2012, February,

Porto, Portugal, 2012.

[12] Faller, Ralf et al. “Preparation, Handover, and Conduction of PRISMA Mission Operations at GSOC.”, 2012.

[13] MONARCH-1 THRUSTER - ArianeGroup, 17 Nov. 2020,
<https://www.ariane.group/en/equipment-and-services/satellites-and-spacecraft/1-n/>.

[14] Anflo, K. and Möllerberg, R., “Flight demonstration of new thruster and green propellant technology on the PRISMA satellite”, *Acta Astronautica*, vol. 65, no. 9, pp. 1238–1249, 2009.

[15] Palmer, Kristoffer et al. “In-Orbit Demonstration of a MEMS-based Micropropulsion system for Cubesats.”, 2016.

[16] T. Grelier, P. -. Guidotti, M. Delpech, J. Harr, J. -. Thevenet and X. Leyre, “Formation flying radio frequency instrument: First flight results from the PRISMA mission,” 2010 5th ESA Workshop on Satellite Navigation Technologies and European Workshop on GNSS Signals and Signal Processing (NAVITEC), 2010.

[17] S. D’Amico, R. Larsson, “Navigation and Control of the PRISMA formation: In-Orbit Experience”, IFAC Proceedings Volumes, 2011.

[18] C. Chasset, S. Berge, P. Bodin, B. Jakobsson, “3-axis magnetic control with multiple attitude profile capabilities in the PRISMA mission,” Proceedings of the 57th IAC/IAF/IAA (International Astronautical Congress), Valencia, Spain, 2006.

13 Appendix

13.1 Mass and power s/s percentages

Subsystem	Comsats ^a		Metsats ^b		Planetary		Other	
	with P/L ^c	GFE P/L	with P/L	GFE P/L	with P/L	GFE P/L	with P/L	GFE P/L
Structure, %	21	29	20	29	26	29	21	30
Thermal, %	4	6	3	4	3	3	3	4
ACS, %	7	10	9	13	9	10	8	11
Power, %	26	35	16	23	19	21	21	29
Cabling, %	3	4	8	12	7	8	5	7
Propulsion, %	7	10	5	7	13	15	5	7
Telecom, %	—	—	4	6	6	7	4	6
CDS, %	4	6	4	6	6	7	4	6
Payload, %	28	—	31	—	11	—	29	—

^aComsat = communication satellite. ^bMetsat = meteorology or weather satellite. ^cP/L = payload.

Figure 38: Mass s/s percentages

Subsystem	Percentage of subsystem total			
	Comsats	Metsats	Planetary	Other
Thermal control	30	48	28	33
Attitude control	28	19	20	11
Power	16	5	10	2
CDS	19	13	17	15
Communications	0	15	23	30
Propulsion	7	0	1	4
Mechanisms	0	0	1	5

Figure 39: Power s/s percentages

13.2 TTMTc theoretical charts

Configuration	Peak gain, dBi	Beam width, deg	Pattern
Helix	$10 \log\left(\frac{D^2 L}{\lambda^3}\right) + 20.2$ (Typically 5 to 20 dBi)	$\frac{16.6}{\sqrt{D^2 L/\lambda^3}}$	
Parabola	$20 \log(\tilde{f}) + 20 \log(D) + 17.8$ (Typically 10 to 65 dBi)	$\frac{65.3\lambda}{D}$	

Figure 40: Antenna experimental formulas

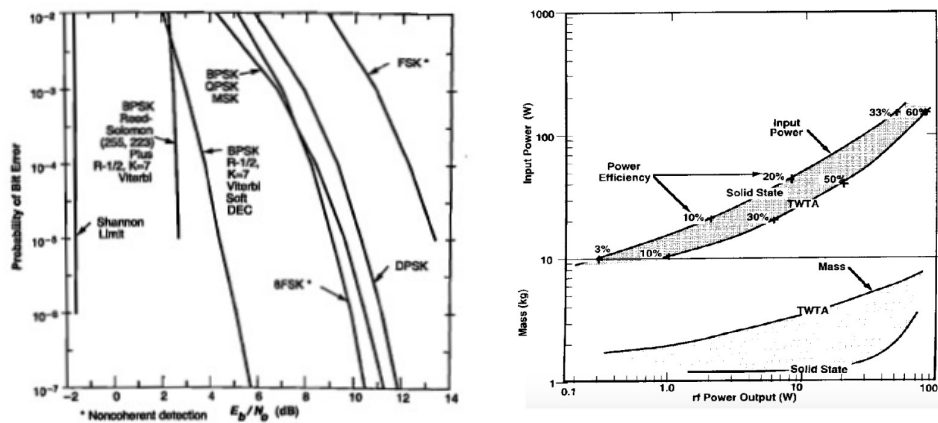


Figure 41: Eb/N0-BER ideal chart, TWTA vs SSA mass and power

13.3 EPS theoretical charts

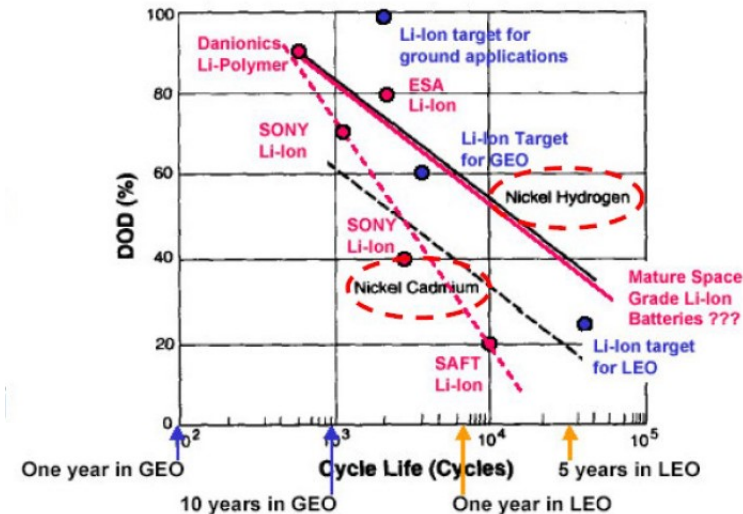


Figure 42: Depth of Discharge - Number of Cycles

13.4 TCS theoretical charts

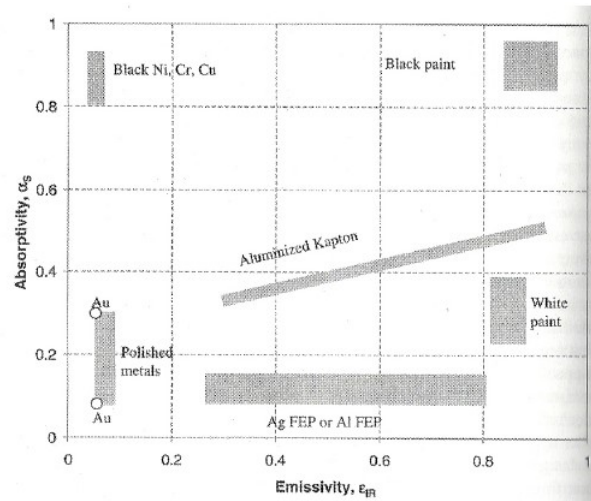


Figure 43: Material properties

13.5 STR theoretical charts

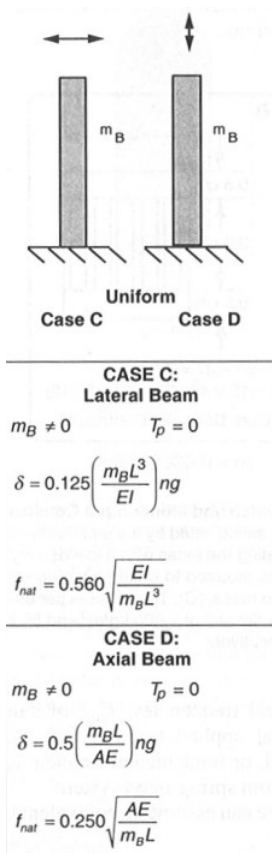


Figure 44: Beam formulas